Geothermics 70 (2017) 110–124

Contents lists available at ScienceDirect

Geothermics

journal homepage: www.elsevier.com/locate/geothermics

Review

Hydraulic performance history at the Soultz EGS reservoirs from stimulation and long-term circulation tests

E. Schill[a,b,*], A. Genter[b,1], N. Cuenot[b,1], T. Kohl[c]

[a] Institute for Nuclear Waste Disposal, Karlsruhe Institute of Technology, Hermann-von-Helmholtz-Platz 1, 76344 Eggenstein-Leopoldshafen, Germany
[b] GEIE "Exploitation Minière de la Chaleur", Route de Soultz – BP 40038, 67250 Kutzenhausen, France
[c] Institute of Applied Geosciences, Geothermal energy group, Karlsruhe Institute of Technology, Kaiserstr. 12, 76131 Karlsruhe, Germany

ARTICLE INFO

Keywords:
Enhanced geothermal systems
Soultz-sous Forêts
Hydraulic yield
Hydraulic stimulation
Engineering advances
Engineering challenges

ABSTRACT

The technical feasibility of Enhanced Geothermal Systems (EGS) has been demonstrated for the first time in fractured crystalline basement rocks at the Soultz-sous Forêts project (France), thus creating a unique and vast data base. At this EGS reference site, different hydraulic and chemical stimulation procedures and experiments were performed in four wells at three different reservoir levels located between 2 and 5 km depth. These measures enhanced significantly the hydraulic yield of the three reservoirs, in some instances by about two orders of magnitude.

In this compilation of hydraulic data, we summarize the achievements at Soultz during the development of three reservoirs by more than 15 major stimulations over a 20-year period between 1988 and 2007. We evaluate the efficiency of the different injection schemes used and provide details on the performance history and testing conditions. In addition to the 52 experiments described for the testing phase, this compilation includes nine tests under operational conditions conducted over the 2008–2013 period.

The evolution of hydraulic yield resulting from various injection, production, and circulation experiments is a major achievement of the Soultz reservoir development. This experience points to two important results: 1) the amount of total volume circulated between wells has a very significant effect on reservoir performance and 2) given the large flow rate variation a common linear trend of pressure increase at higher fluid flow rates develops that manifests over all three reservoirs. A strong focus is on the well tests in the intermediate reservoir allowing for a characterization of productivity and injectivity indices. Our analysis showed that initial hydraulic conditions from single-well injection tests are comparable to each other in the three reservoirs, but individual fault zones may determine the stimulation behaviour. We identify progressive cyclic injection in combination with circulation between wells reaching high hydraulic yields at comparatively low pressure. The Soultz data suggest how to maximize injection and minimize induced seismicity. This unique data base illustrates the learning curve achieved in Soultz and provides a strong basis for further conceptual model developments.

1. Introduction

The International Energy Agency aims at a world-wide increase in renewable electricity production using geothermal energy from presently about 10 GW_e to 140–160 GW_e installed capacity by 2050 (IEA, 2011). Part of this growth is expected to be covered by Enhanced Geothermal Systems (EGS), whose current capacity of about 10 MW_e would grow by more than four orders of magnitude, reaching 70–90 GW_e by 2050. Against this background, what was learned at the EGS test site at Soultz-sous-Forêts (France) in the Upper Rhine Graben (e.g., Gérard et al., 2006), has contributed significantly to the reservoir engineering and operational aspects of these systems. Along the Soultz learning curve, a number of milestones in reservoir stimulation have been reached. The objective of the present review is to highlight and reappraise these major achievements.

At Soultz, EGS development comprises crystalline basement rock and extends over three reservoir levels; i.e., at 2000 m depth (R2, at the top of the granitic basement), at 3500 m (R3), and at 5000 m (R5). About 15 major hydraulic and chemical stimulations were carried out to improve reservoir condition at those different levels. The shallowest reservoir lying at 1200 m (R1) in the Triassic sediments has shown some occurrences of partial or total mud losses related to fractures

* Corresponding author.
E-mail addresses: eva.schill@kit.edu, eva.schill@stw.de (E. Schill).
[1] Now at: ES-Géothermie, 5 rue de Lisbonne, Bâtiment Le Belem, 67300 Schiltigheim, France.

http://dx.doi.org/10.1016/j.geothermics.2017.06.003
Received 17 February 2016; Received in revised form 24 April 2017; Accepted 5 June 2017
Available online 26 June 2017
0375-6505/

zones during drilling operation (Vidal et al., 2015). R1 was never hydraulically tested or stimulated. During nine periods in 1997, 2005 and between 2008 and 2013, long-term productivity was demonstrated in R3 and R5. The deepest reservoir (R5) was developed to ensure electricity production.

EGS technology has been advanced further in follow-up projects such as at Landau (Germany), Insheim (Germany), and Rittershoffen (France, e.g., Baujard et al., 2017). At these sites, the concept of enhancing the naturally most productive reservoir level at the top of the granitic basement was applied, as well as specific hydraulic stimulation techniques (e.g., Schindler et al., 2010).

Monitoring hydraulic performance development in a reservoir is typically based on different types of hydraulic tests. At Soultz, in the initial phase of engineering of the different wells, mostly injectivity index (JI) was determined, while at more advanced stages depending on the performance of the well, productivity index (PI) is tested. Typically at Soultz, PI and JI were measured at single wells, i.e. without pressure measurement in a second well. It is important to note that the present evaluation of Soultz tests is strongly related to an engineering approach based on simplified hydrogeological concepts consisting of representative elementary volumes of a single fracture and the surrounding matrix (Bear, 1972). During the development phase, JI and PI were determined using

$$JI \text{ or } PI = \frac{Q}{\Delta P}$$

where Q is the flow rate and ΔP is pressure difference obtained at quasi-stationary conditions downhole. IJ and PI are summarized under the term hydraulic yield (HY) or reversely, the hydraulic impedance. For specific test condition, we refer to the original reports and publications listed in Annex A. Furthermore, it would exceed the scope of this paper to compile the complex conceptual models developed (e.g., Baujard and Bruel, 2006; Kolditz, 2002) that are relevant to understanding the details of effects of massive injections in a heterogeneous fractured medium by accounting for the importance of the coupling between the thermo-hydraulic-mechanical-chemical (THMC) processes.

At Soultz, the naturally fractured and engineered R5 fulfils most of the EGS criteria established by Garnish (2002 Table 1). R5 has been enhanced between 2000 and 2005 using different chemical and hydraulic stimulations and further improved by circulation during operation. Until 2013, when a major restructuring started at Soultz, this site was run as a multi-well and multi-reservoir experiment. The contribution of natural hydrothermal fluids to total production is of about 75 % (Sanjuan et al., 2006).

In the framework of developing new environmentally friendly stimulation and circulation concepts, this study comprises a total of 61 tests and circulation experiments and aims at providing general conclusions for EGS reservoir engineering. It summarizes and compares the

Table 1
Definition of Enhanced Geothermal System (EGS) by reservoir parameters (Garnish, 2002) in comparison with the R5 parameter of Soultz-sous-Forêts from 2011 (Cuenot et al., 2011). .

	EGS definition	2011 R5 parameters
Flow rate	50–100 kg s^{-1}	23 L s^{-1}
Mean wellhead fluid temperature	150–200 °C	157.5 °C
Effective heat exchange area	> $2{\cdot}10^6$ m^2	n/a
Rock volume	> $2{\cdot}10^8$ m^3	about $2.7{\cdot}10^9$ m^3
Hydraulic impedance	< 0.1 MPa kg^{-1} s^{-1}	0.1 MPa L^{-1} s^{-1} (GPK1, inj.) 0.05 MPa L^{-1} s^{-1} (GPK2, prod.) 0.25 MPa L^{-1} s^{-1} (GPK3, inj.; GPK4, prod.)
Water loss at the surface	< 10 %	0% (total reinjection)

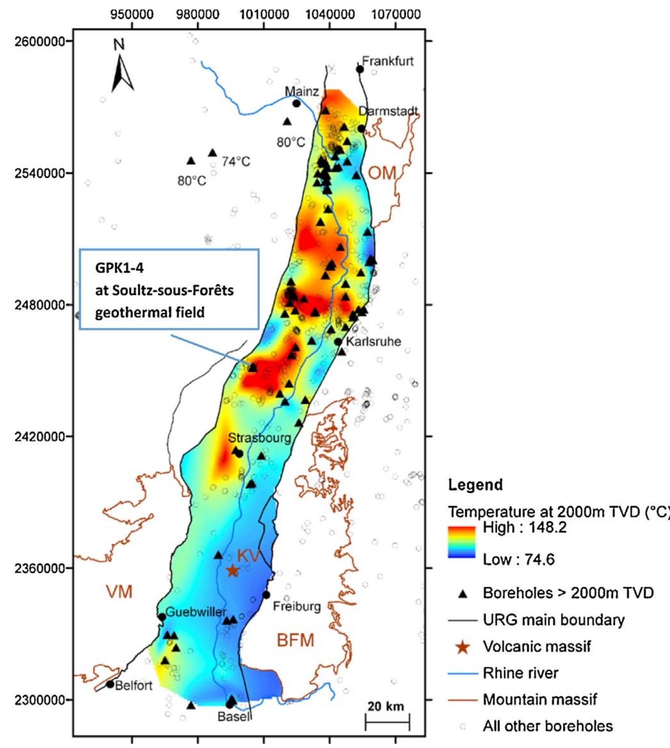

Fig. 1. Temperature distribution at 2000 m TVD in the Upper Rhine Graben, URG, (modified after Baillieux et al., 2013) based on (Agemar et al., 2012). Boreholes with depths > 2000 m TVD are indicated by triangles. VM: Vosges mountains; BFM: Black Forest mountains; OM: Odenwald mountains; KV: Kaiserstuhl Volcanic massif. Lambert II coordinates.

conditions and effectiveness of the major stimulations performed at Soultz between 1988 and 2007 that to date are mainly published in internal reports and found in the project's archives. Additionally, we provide a summary and present new data on circulation experiments up to 2013. The study adds to an earlier assessment of Nami et al. (2008) that discussed the reservoir enhancement resulting from chemical stimulation operations in the deep reservoir suggesting that chemical stimulation of different types may contribute more than 50% of the post-stimulation PI.

This first comprehensive compilation of the performance across all reservoirs includes the key information for all hydraulic operations during development and operation phase at Soultz. It is part of a 4D object-oriented database launched by GEIE Exploitation Minière de la Chaleur and the University of Strasbourg (Jahn et al., 2017).

2. Natural geothermal and hydraulic settings

The Soultz EGS site is located in the central Upper Rhine Graben (Fig. 1), where local subsurface temperature maxima with thermal gradients up to > 100 K km^{-1} in the sedimentary cover of the Variscan crystalline basement, provide favourable condition for geothermal utilization (Genter et al., 2003). The origin of these temperature anomalies has been attributed to free convection along the major faults (Bächler et al., 2003 ; Kohl et al., 2000) that supported hydrothermal circulation in the crystalline basement at the graben scale (Baillieux et al., 2014; Guillou-Frottier et al., 2013; Pribnow and Schellschmidt, 2000; Schellschmidt and Clauser, 1996). At depths > 3700 m the temperature gradient recovers from < 10 K km^{-1} to a normal geothermal gradient of 30 K km^{-1} (Pribnow and Schellschmidt, 2000). Maximum temperature of 201 °C is reached at 5097 m bottomhole depth in GPK2.

The spatial relationship between temperature anomalies and neotectonic patterns indicates a compressional shear and uplift regime for the major thermal anomalies of the central segment of the graben (Illies

Table 2
Development of the three reservoir levels (R2, R3 and R5) with corresponding stimulated reservoir sections (m TVD) and natural JI ($m^3 s^{-1} MPa^{-1}$) with complete openhole sections (m MD) of the wells EPS1 and GPK1-4 at the Soultz-sous-Forêts EGS site (Hettkamp et al., 2004; Jung, 1992; Jung et al., 1995; Tischner et al., 2007; Weidler, 2001).

	EPS1	GPK1	GPK2	GPK3	GPK4
R2 (1400–2200 m)	n/a (1990 – 2227)	$9{\cdot}10^{-4}$ (1965 – 1999)	$2{\cdot}10^{-1}$ (2098)		
R3 (3000–3900 m)		$5{\cdot}10^{-4}$ (2845 – 3574)	$3{\cdot}10^{-4}$ (3205 – 3870)		
R5 (4000–5400 m)			$2{\cdot}10^{-4}$ (4403 – 5026)	n/a (4488 – 5021)	$1{\cdot}10^{-4}$ (4479 – 4972)

and Greiner, 1979). Approximately N-S to NE-SW trending normal faults caused general deepening of the top of the crystalline basement towards the East during the formation of the graben. The local structural setting at Soultz is strongly influenced by a horst structure. As a consequence, the top of the crystalline basement was encountered at relatively shallow depth at the Soultz site (about 1400 m). It is composed of two main granites with a lithology change at about 4700 m depth that partly coincides with the vertical boundaries of the three reservoir levels (Genter et al., 1999). The upper part (from 1420 to 4700 m) is referred to as potassium feldspar granite. An about 100 m thick alteration zone at its top appears in different geological and geophysical characterizations, such as a zone of low magnetic susceptibility (Rummel and König, 1991) construed as paleo-weathering. It is characterized by high electric conductivity (Geiermann and Schill, 2010) interpreted to be caused by hydrothermal alteration, and high values of heat production of up to 7 μW m^{-3} (Grecksch et al., 2003; Pribnow, 2000). Below, this part includes an upper fracture cluster at 1800–2000 m depth in unaltered porphyritic granite with a mean fracture density of about 1 m^{-1} (Dezayes et al., 2005). Further down, a number of naturally permeable zones were identified by significant mud losses during drilling (Dezayes et al., 2010). Below, the potassium feldspar granite includes a highly altered and fractured intermediate section (between about 2700 and 3900 m) with mean fracture density of 0.4 m^{-1} and maxima up to 2.86 m^{-1} (Dezayes et al., 2005). Typically, fracture zones with an enhanced tendency to shear during stimulation fit with the occurrence of hydrothermally altered and fractured zones (Evans et al., 2005; Genter et al., 1999; Meller et al., 2014). The deeper part of the basement (from 4700 to 5000 m) corresponds to a fine-grained two-mica granite with a mean fracture density of 0.6 m^{-1} and maxima of up to 1.97 m^{-1} (Dezayes et al., 2005).

The total vertical extension of the reservoirs (Table 2) has been determined from the distribution of the seismic clouds during stimulation (Beauce et al., 1992; Cuenot et al., 2011; Jones et al., 1995). It should be mentioned that in the well GPK1, R2 and R3 appear to be connected. The seismic clouds during stimulation of R5 reveal a maximum reservoir depth of about 5400 m. R2 was assessed through the well EPS1 to a depth of 2227 m, as well as GPK1 to a depth of 2000 m. A test during drilling operation of GPK2 has been carried out in R2 at the 2098 m depth level. R3 was developed between GPK1 and GPK2 that at the time had reached depths of 3590 m and 3876 m, respectively. R5 includes wells GPK2, GPK3 and GPK4.

In the following, we will use indices R2 to R5 and G1-G4 to indicate the different reservoir levels and wells GPK1 to GPK4. The natural undisturbed hydraulic condition prior to stimulation arising from these fracture settings are summarized in Table 2 for the three reservoir levels R2 to R5 including their corresponding openhole sections.

Undisturbed JI in the different reservoirs were determined before stimulation in single-well injection tests (Jung, 1992; Jung et al., 1995; Tischner et al., 2007; Weidler, 2001). They generally reveal similar values for R2 and R3 with mean $JI_{R2\text{-}R3,G1\text{-}G2} = 6{\cdot}0^{-4}$ $m^3 MPa^{-1} s^{-1}$ (Table 2; Fig. 2). Exceptionally high $JI_{R2,G2} = 0.2$ $m^3 MPa^{-1} s^{-1}$ was determined in R2 at 2100 m depth in the pre-stimulation test 95FEB02 for a fracture zone causing total mud losses during drilling of GPK2 (Jung et al., 1996). Given the lateral extension of the microseismic clouds (Jones et al., 1995), an influence of prior stimulations of GPK1 on this value cannot be totally excluded.

Comparably lower undisturbed single-well JI are observed in R5 $JI_{R5,G2\text{-}4} = 1\text{-}2{\cdot}10^{-4}$ $m^3 MPa^{-1} s^{-1}$ from GPK2 and GPK4 (Tischner et al., 2007; Weidler, 2001). JI for GPK3 has never been determined under single-well conditions. Its $PI_{R5,G3} = 2{\cdot}10^{-3}$ $m^3 MPa^{-1} s^{-1}$ appears to be one order of magnitude higher than JI observed in GPK2 and GPK4 (Hettkamp et al., 2004). It has been determined in conjunction with injection into GPK2 and that the openhole section had reached the already stimulated part of the reservoir during drilling.

Taking into account single-well tests, only, and excluding the anomalous large $JI_{R2,G2}$, an undisturbed JI decrease with increasing

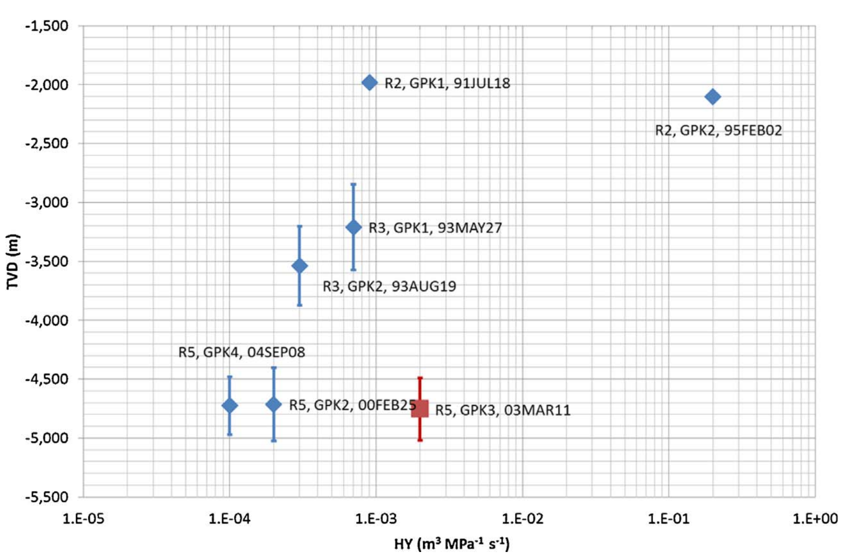

Fig. 2. Hydraulic yield (HY) of ambient, non-stimulated R2 to R5, acquired in single-well injection tests (blue) at GPK2 and GPK4 and under circulation and production conditions (red) in GPK3. (For interpretation of the references to colour in this figure legend, the reader is referred to the web version of this article.)
Data source: see Annex A. Vertical bars indicate the vertical extension of the respective openhole sections (true vertical depth below ground, TVD).

Table 3
Outline of the major injection and production periods (including hydraulic stimulation) in the three reservoir levels R2 to R5 a) in the reservoir development stage including the according open-hole sections of the different wells in m MD, and b) the operation phase. Further details are given in Annex A.

a)

	1988	…	1991	1993	1994	1995	1996	1997	…	2000	…	2003	2004	2005	2006	2007
R2	$JI_{R2,G1}$ 1,966-2,000m															
R3				$JI_{R3,G1}$[a] 2,850-3,590m[b]		$PI_{R3,G1}$[c] 2,850-3,590m	$JI_{R3,G1}$[e] 2,850-3,590m									
						$JI_{R3,G2}$[d] 3,211-3,876m	$PI_{R3,G2}$[e] 3,211-3,876m									
R5										$JI_{R5,G2}$[f] 4,431-5,084m		$PI_{R5,G2}$[f]				
												$JI_{R5,G3}$ 4,558-5,102m				
													$JI_{R5,G4}$ 4,758-5,261m	$PI_{R5,G4}$[g]	$JI_{R5,G4}$	

[a]94JUN16: $PI_{R3,G1}$
[b]93SEP01: 2,850-3,400m
[c]95JUL09-96SEP28
[d]95JUN16-96SEP28
[e]from 96OCT13
[f]to/from 03JUN10
[g]05JUL11

b)

	2008	2008	2009	2010	2011	2011	2012	2013
R3			$JI_{R3,G1}$	$JI_{R3,G1}$	$JI_{R3,G1}$	$JI_{R3,G1}$	$JI_{R3,G1}$	$JI_{R3,G1}$
R5	$PI_{R5,G2}$	$PI_{R5,G2}$	$PI_{R5,G2}$	$PI_{R5,G2}$	$PI_{R5,G2}$	$PI_{R5,G2}$	$PI_{R5,G2}$	$PI_{R5,G2}$
	$JI_{R5,G3}$	$JI_{R5,G3}$	$JI_{R5,G3}$	$JI_{R5,G3}$	$JI_{R5,G3}$	$JI_{R5,G3}$	$JI_{R5,G3}$	$JI_{R5,G3}$
		$PI_{R5,G4}$	$PI_{R5,G4}$				$JI_{R5,G4}$	$JI_{R5,G4}$

depth cannot be excluded for the granitic basement at Soultz. So far, such observations have been made for the hydraulic conductivity of the gneissic basement world-wide (Ingebritsen and Manning, 1999), but seem to be less evident for granitic basement (Stober and Bucher, 2007). It should be mentioned that JI values > $5{\cdot}10^{-4}$ m^3 MPa^{-1} s^{-1} apply to dominant single fractures or faults and that average granite shows values < $1{\cdot}10^{-4}$ m^3 MPa^{-1} s^{-1}.

During the development of the Soultz EGS project, different measures have been taken with the aim to improve the hydraulic yields in the different reservoirs and wells between 1988 and 2013. An overview of the major stimulation experiments and tests including production and injection periods between 1988 and 2007 is given in Table 3a, with corresponding values in Annex A. In R2 and R3 only hydraulic stimulations were conducted (Jung, 1992; Jung et al., 1996; Jung et al., 1995). In the wells of R5, hydraulic stimulations were followed by, or combined with, additional chemical stimulation (Baria et al., 2000; Gérard et al., 2006; Hettkamp et al., 2004; Tischner et al., 2007; Weidler et al., 2002). Between 2005 and 2013, a number of eight long-term circulations (Table 3b) have been carried out between wells GPK2 to GPK4 in R5, partly combined with R3 involving well GPK1 (Annex B). The following sections provide more detailed analyses of the testing conditions. Volume (V), flow rate and the resulting differential reservoir pressure increase are used to hydraulically characterize the reservoirs.

3. Hydraulic stimulation history of GPK1 and GPK2 in the intermediate reservoir R3

3.1. Reservoir setting

R3 was engineered through the wells GPK1 and GPK2 with open-hole sections of 740 m measured depth (MD) and 665m MD between 2850–3590 m MD and 3211–3876 m MD, respectively (Baria et al., 1995). At these depths, the two wells are about 450 m apart from each other (Fig. 3a, b). R3 was hydraulically stimulated first in 1993 through GPK1 (Annex A). GPK2 was drilled into the outer part of the seismic

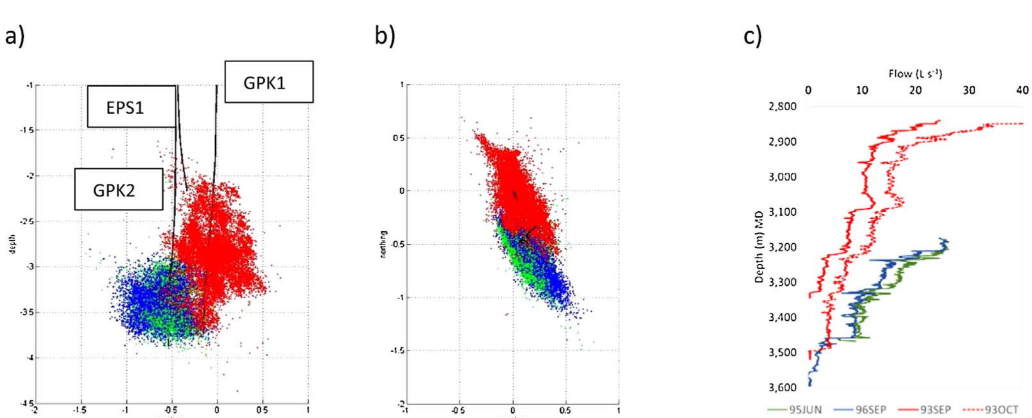

Fig. 3. Microseismic events (a, b) and flow logs during injection experiments (c) during different stimulation experiments in R3 including the stimulations of 1993 (red), 1995 (green) and 1996 (blue). The green line represents the well path of EPS1. Soultz coordinate system (km). Full/dashed line: 25 L s^{-1}/41 L s^{-1}-injection. (For interpretation of the references to colour in this figure legend, the reader is referred to the web version of this article.)

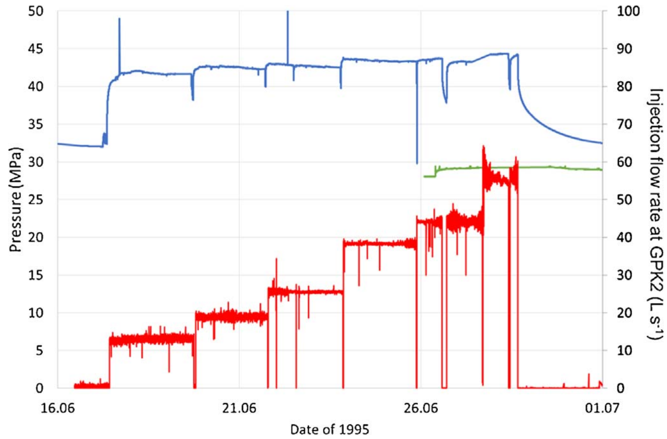

Fig. 4. Injection flow rate (red) and development of reservoir pressure (blue: GPK2; green: GPK1) during 95JUN16 to 95AUG09 experiments in GPK1 and GPK2 (Baumgartner et al., 1996). While in GPK1 the production was shut-in the late stage of the experiment, pressure build-up in GPK2 is due to the injection. In contrast to conventional injection experiments (e.g., 95JUL09) with a continuous stepwise increasing flow rate, injection in the 95JUN16 experiment injection was stopped and pressure released after each incremental increase of the flow rate in order to acquire flow logs. (For interpretation of the references to colour in this figure legend, the reader is referred to the web version of this article.)

clouds recorded during the 1993 injections and stimulated in 1995 and 1996 (Annex A). For GPK1 a connection between R2 and R3 is indicated by the events induced by the stimulations 93SEP01 and 93OCT11 (Fig. 3a, b). The bottom of well EPS1 is located within this 1993 seismic cloud, although showing a lower density of events compared to GPK1 at the same depth. Also, a fault zone cutting GPK1 between 2710 and 3050 m depth has been observed in vertical seismic profiles. This fault zone passes just below the bottom of EPS1 (Place et al., 2010).

In contrast to the possible connection between EPS1 and GPK1, the connectivity between GPK1 and GPK2 has been successfully tested by different tracer tests during circulations 95JUL09, 95AUG01, 95AUG15 and 97JUL12 (Aquilina et al., 1998). Notwithstanding complete tracer loss during the first 10 kg fluorescein pulse, fluid-chemistry indicates a hydraulically connected fracture network without short circuit between the two wells (Aquilina et al., 1997). During the long-term circulation test (97JUL12) tracer injection characterized the flow field. Benzoic acid and fluorescein peaks arriving after 144–240 h indicate that the reservoir volume increased during 97JUL12 circulation and correlates with the main flow path between the two boreholes (Aquilina et al., 2004). This flow path is related to the fractured zones below the casing (2850 to 2950 m in GPK1, and 3200 to 3360 m in GPK2) that were enhanced by stimulation and absorbed 65% of the flow. A pressure drop in the long-term circulation experiment 97JUL12 from 3.5 to 2 MPa has been related to a flow redistribution (logged at 97NOV15) connected to a single large fracture zone at 2860 m (approximately 10 m below the casing shoe) increasing its hydraulic yield by nearly 100%. It accounts now for 44% of the total flow into the reservoir (Baumgartner et al., 1998). The high deuterium peak (at 430 h) is related to the specific flow path of the 3500 m-deep fracture zone where deuterium was injected. These fractures show indications of natural permeability during drilling operations (Genter et al., 1995), which was confirmed by Jung et al. (1995), when plugging the lower part of the GPK1 openhole section to a depth of 3400 m led to a reduction of the $JI_{R3,G1}$ by one order of magnitude. A total of 25–35% of the injected benzoic acid and fluorescein was recovered until the end of the test. A conservative estimate indicates a minimum of 65% of natural brine contribution to the produced fluid. The fracture aperture calculated from tracer break-through volumes is 2.9 10^{-2} m, whereas hydraulic aperture determined from transmissivity is about 2.6 10^{-4} m (Jung, 2013).

Fracture zones appear to be responsible for the high transmissivity in the openhole sections in GPK1 and GPK2 (Fig. 3b). The connection to tectonic structures became evident, as post-stimulation spinner-log flow tests (Baumgartner et al., 1996, 1998) reveal five hydraulically significant fractures in GPK1 between 2850 and 2960 m MD (Evans et al., 2005) below the casing shoe that take up about 60% of the flow. Additionally, fractures at 3230 and 3490 m MD take up about 22% and 15% of the fluid, respectively. These fractures are also observed in the composite logs (Dezayes et al., 2010). The impact of the 93SEP01 hydraulic stimulation on the single fractures in GPK1 was evaluated in detail by Evans et al. (2005). Permeability enhancement was found to be limited to hydrothermally altered sections. In GPK2 fracture zones at 3240, 3350 and 3515 m MD identified in the composite logs with respective thicknesses of about 0.5 m, 3 m and 12 m (Dezayes et al., 2010) appear to be hydraulically active (Fig. 3b). Flow distribution along the openhole sections reveal about 30% around 3240 m and 3350 m MD at about 20% around 3515 m MD during the 95JUN16 stimulation. Major flow redistribution occurs during 96SEP18 stimulation at around 3240m.

3.2. Impact of test conditions on hydraulic yield

Due to changes in the boundary condition, single-well injection and production or multi-well test configurations with circulation condition should be first characterized individually. In the framework of the current review, R3 was selected as the most representative example from Soultz since intensive testing was performed without chemical treatment.

In R3, five hydraulic stimulations were carried out successfully between 93SEP01 and 96SEP18 (Annex A) in the openhole sections of GPK1 and GPK2. Two stimulation tests 93AUG19 and 93OCT01 failed due to problems in isolating the lower part of the openhole using packers. Single-well stimulations were conducted in 1993. The experiment 93SEP01 was intended to stimulate the weakly fractured matrix of the upper openhole section by plugging its highly permeable lower part between 3400 and 3590 m MD.

GPK2 has been stimulated together with production from GPK1 in the initial phase in 95JUN16 and 96SEP18. In 95JUN16, initially 300 m^3 of heavy brine with a density of 1180 kg m^{-3} were injected and gradually diluted by adding fluid that was produced in GPK1 (Baumgartner et al., 1996). GPK1 is used as producer up to the 44 L s^{-1}-step and then shut-in. In GPK2, a shut-in phase was inserted at each interval leading to a decrease of wellhead pressure between 2 and 5 MPa before stepping up flow again (Fig. 4). In 96SEP18, 12 L s^{-1}-production from GPK1 (3700 m^3) was limited to the first 25 L s^{-1}-injection step (Jung, 1999). Afterwards, injection was increased in two steps to 45 and 78 L s^{-1}.

The history and development of the hydraulic yield of GPK1 experiments are shown in Fig. 5. The various hydraulic tests of GPK1 allow comparing the impact of single-well injection or production testing to circulation conditions, involving injection into EPS1 or GPK2. Initial $PI_{R3,G1}$ and $JI_{R3,G1}$ determined in the single-well tests 93MAY27 and 93AUG19 are in the same range. During the first step test in 93SEP01, starting from natural matrix condition of $JI_{R3,G1} = 5{\cdot}10^{-5}$ m^3 MPa^{-1} s^{-1}, JI has increased to $JI_{R3,G1} = 6{\cdot}10^{-4}$ m^3 MPa^{-1} s^{-1} when employing $\Delta P = 9$ MPa at 18–36 L s^{-1}. This value corresponds to the initial JI and PI range determined across the entire openhole section including natural permeable fractures in 93MAY27 and 93AUG19. After stimulation of the entire openhole section in 93OCT11, flow rate reached 35 L s^{-1} at ΔP of 10 MPa leading to a total $JI_{R3,G1} = 1{\cdot}10^{-3}$ m^3 MPa^{-1} s^{-1}. This corresponds to an increase by a factor > 10 compared to the initial natural $JI_{R3,G1}$ (93AUG19) of the entire openhole section.

In the 94JUN16 production test, a volume of 6200 m^3 was circulated with re-injection into EPS1. The ΔP of 3.4 MPa at flow rates of 18.5 L s^{-1}

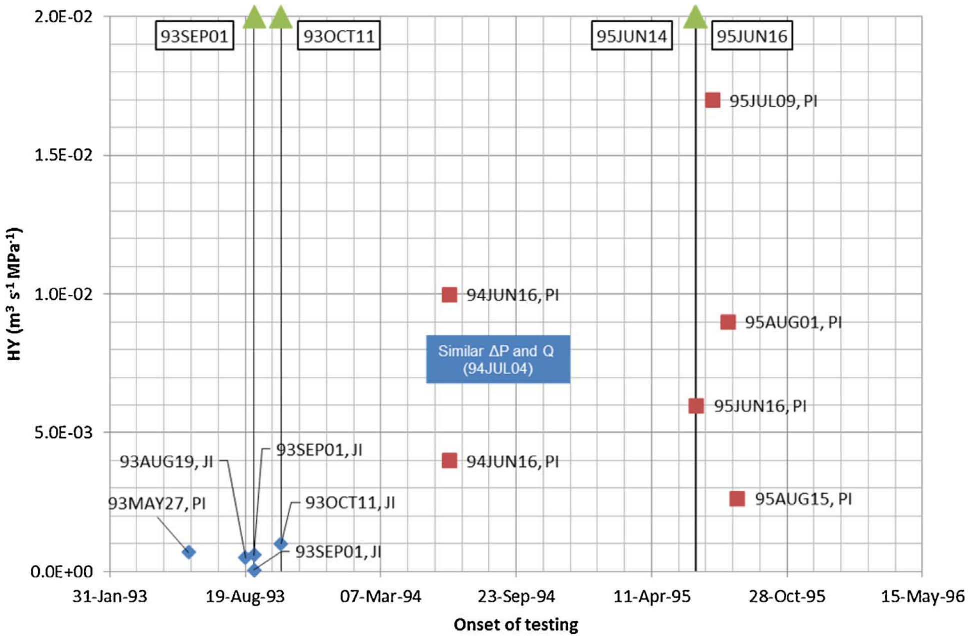

Fig. 5. Development of $JI_{R3,G1}$ and PI $_{R3,G1}$ from-single-well injection tests and circulation production tests in GPK1 (blue: single-well tests, red: circulation condition, green: hydraulic stimulations). During circulation GPK1 was used as producer with re-injection in EPS1 (94JUN16) and in GPK2 (95JUN16; 95JUL09; 95AUG01; 95AUG15). Simultaneous tracer tests were carried out over the entire periods of the 95JUL09, 95AUG01, and 95AUG15 tests.
Data source: see Annex A.

were interpreted as $0.4 \cdot 10^{-4} < PI_{R3,G1} < 1 \cdot 10^{-4}$ m^3 MPa^{-1} s^{-1} by Hettkamp et al. (2004) and Jung et al. (1995), respectively. Similar values were found in: 1) the single-well injection test 94JUL04 at identical ΔP/flow rate of 18 L s^{-1} (Jung et al., 1995) and 2) the first, low-pressure step of the GPK2 stimulation 95JUN16 at a flow rate of 12 L s^{-1} and ΔP of 5 MPa involving production from GPK1 (Hettkamp et al., 2004). At this point it seems that $IJ_{R3,G1}$ and $PJ_{R3,G1}$ are comparable at different test conditions. However, with the exception of 94JUL04 single-well test, a significant increase in hydraulic yield is observed between single-well test 93OCT11 $JI_{R3,G1}$ and circulation test 94JUN16 $PI_{R3,G1}$. Maximum hydraulic yield is observed in the 95JUL09 production test, after having injected and produced more than 40 days in this well.

Stimulation experiments in GPK2 started in 1995. The respective hydraulic yields for GPK2 are shown in Fig. 6. The initial hydraulic yield of GPK2 determined in the tests 95FEB02 and 95JUN14 are comparable to the values of GPK1. After a first short stimulation (95JUN14) at flow rates of 30 L s^{-1} and ΔP of 12.2 MPa, the 95JUN16 test was carried out (Jung, 1999). A step-rate injection test conducted after stimulation (95JUL01) indicated that the impedance to flow had been substantially reduced, but was now turbulent-like (Kohl et al., 1996). Reverse flow was applied in GPK2 in the 96AUG14 experiment after fractures with high JI in this well had been progressively plugged during test 95AUG15 by re-injecting unfiltered brine into GPK2, and $PI_{R3,G1}$ had dropped to $2.6 \cdot 10^{-3}$ m^3 MPa^{-1} s^{-1} (Gérard et al., 1997). Flow condition were re-established at the end of this test, when $PI_{R3,G2}$ reached $1.4 \cdot 10^{-2}$ m^3 MPa^{-1} s^{-1}. A second massive stimulation of GPK2 was performed in 96SEP18. In this stimulation, one of the largest volumes ever used for stimulation in Soultz, 27,000 m^3 were injected at flow rate steps from 25 to 78 L s^{-1} (Gérard et al., 1997). During this experiment $JI_{R3,G2}$ was slightly increased. The follow-up 96SEP29 test showed that the flow remained turbulent-like (i.e., non-Darcian).

The hydraulic yield of the single-well production test 96AUG14 was

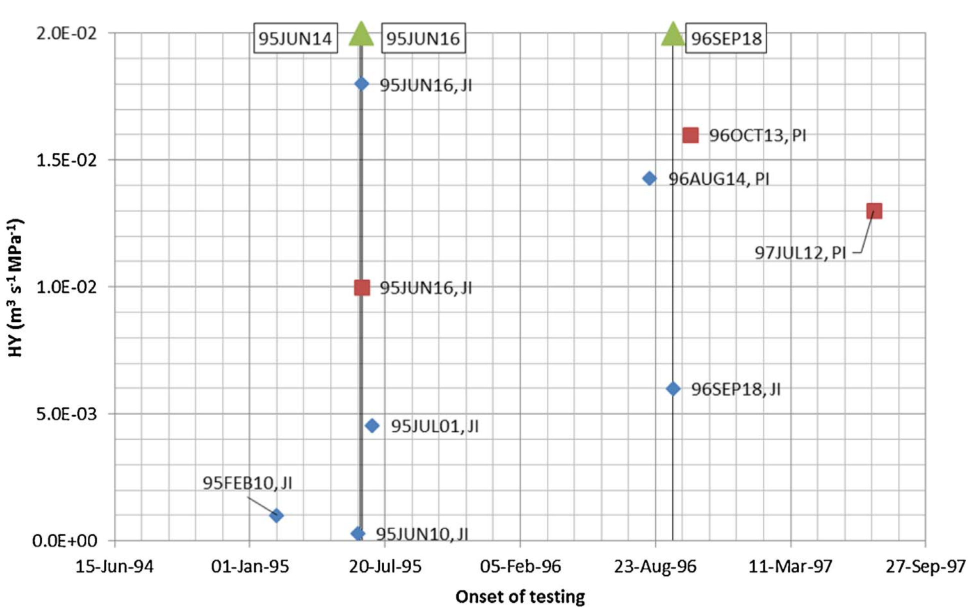

Fig. 6. GPK2 experiments with $JI_{R3,G2}$ and PI $_{R3,G2}$ measured during single-well injection tests (95FEB10, 95JUN10, 96SEP18, 96SEP29), single-well production test (96AUG14) and circulation production tests after 95AUG15 (96OCT13, 97JUL12) (blue: single-well tests, red: circulation condition, green: hydraulic stimulations). Tests during 95JUN16 stimulation have been attributed to circulation condition at the beginning of the stimulation, when production occurred in GPK1, and to single-well condition at the end of the test, when pressure was shut-in GPK1.
Data source: see Annex A.

confirmed by $PI_{R3,G2}$ of 96OCT13 and 97JUL12, which were carried out under circulation conditions. $JI_{R3,G2}$ (96SEP18) is clearly lower compared to the values of $PI_{R3,G2}$, when measured under single-well condition.

It can be summarized that the hydraulic stimulation of R3 between 1993 and 1996 was very successful. Furthermore, different observations open perspectives to further investigation on the nature of the fracture pathways involved. In the context of the general observation of differences in PI and JI (e.g., O'Sullivan and Pruess, 1980), the initially quite similar values of JI and PI in R3 confirm the experience from other liquid-phase reservoirs worldwide (Garg and Combs, 1997). Starting from identical values in 1993, the two stimulations of GPK1 showed an increase of first of $PI_{R3,G1}$ that were later confirmed for $JI_{R3,G1}$ for 94JUL04 (Fig. 5, Jung et al., 1995). Being used as producer only without further stimulation, the subsequent history of $JI_{R3,G1}$ for 1995 is not documented here. The similarity in hydrogeological parameters is also supported by sophisticated non-Darcian flow analyses (Kohl et al., 1997). In GPK2, $PI_{R3,G2}$ is constantly high between 96AUG14 and 96SEP18 and maintained stable at the circulation of 97JUL12. It may be noted that non-Darcian flow was also postulated in the interpretation of the 95JUN16 stimulation in GPK2. It describes the characteristic pattern of R3 with successful near borehole stimulation, but without affecting impedance at larger distances. The assumption of matrix impedance is also supported by the missing breakthrough of the tracer injected at this stage. At a later phase of GPK2 stimulation in R3 starting 96SEP18, differences between PI and JI appear (Fig. 6), showing the expected pattern with lower JI, possibly due to plugging from cuttings at the injector.

In terms of efficiency of reservoir engineering, similar stimulation flow rates and volumes lead to similar hydraulic yields in GPK1 and GPK2 (under circulation conditions). Against this complex background, the question of the driving parameters for efficient stimulation remains.

4. Full reservoir stimulation and circulation behaviour

4.1. Stimulation overview

In Annex A, all 55 archived hydraulic tests performed over the reservoir creation period between 1988 and 2007 in the three reservoirs of Soultz are detailed and referenced to publically available or original reports. For each test its name, reference, well(s) and injected/produced depth range are given. In addition, the hydraulic yield, injected chemical additives, and the "total single-test volume, ΣV" (i.e. the total volume injected or produced during a specific test with injection having positive and production having negative signs) and the "total fluid flow volume, ΣTV" (i.e. the total volume injected or produced at a specific borehole interval over the years without differentiation between injection or production) are given. The single- and multi-step tests are characterized by flow rate, differential down-hole pressure (where available) and approximate test duration for the individual steps. They can be specified as following:

- **R2**: Five injection tests, with four JI determined, only single-step tests
- **R3**: 21 tests (incl. nine circulation tests) with nine JI and nine PI determined partly under circulation conditions. Nine multi-step tests were conducted.
- **R5**: 29 tests (incl. four circulation tests and seven tests including chemical additives) with 17 JI and eight PI determined partly under circulation conditions. 11 multi-step tests were conducted.

The complexity of the test conditions has increased over time. Starting in 1988 only single-well and single-step tests have been conducted in R2. In R3, many multi-step tests involving more than one well were carried out. Finally, during the period 2005–2007, multi-step tests were carried out also with strong chemical reactants in R5. The maximum pressure in Soultz of 19 MPa was measured for 48 h during 05MAR02 in GPK4 (see Baria et al., 2005). Neglecting the short-peak injection ($\Delta t < 3$ h) of 03MAY27, a maximum long-term flow rate of 78 L s^{-1} was injected in 96SEP18 at R3 in GPK2. Highest yield was estimated at R2 in GPK2 with JI = $2{\cdot}10^{-1}$ m^3 MPa^{-1} s^{-1} under ambient conditions (see Section 2, test conducted in 95FEB02 during drilling operations).

Final hydraulic yields in the different reservoir levels range from about $5{\cdot}10^{-3}$ m^3 MPa^{-1} s^{-1} in R5 to $> 1.5{\cdot}10^{-2}$ m^3 MPa^{-1} s^{-1} in R3. Major improvement in reservoir enhancement (Table 4) by approximately a factor of 10 was confirmed in the hydraulic tests 91JUL18 in R2. In R3, improvement factors of about 30–50 have been achieved in 95JUN16 and 96OCT13 and confirmed in the long-term circulation test 97JUL12. An improvement factor of 50 was reached in the circulation test of 03JUN24 in GPK2 in R5. Except from the contribution of the 03FEB12 acidification with maximum flow rates of 30 L s^{-1} and a total injection volume of 1460 m^3, all major enhancements were obtained by hydraulic stimulation, only. In R3 and R5, all maximum hydraulic yields have been observed in the respective production wells and under circulation conditions.

Table 4
Comparison of ambient and maximum hydraulic yields, HY (m^3 $MPa^{-1}s^{-1}$), in the three reservoir levels R2 to R5 at the Soultz-sous-Forêts EGS site.
Data source: see Annex A.

Reservoir	Well	Test ambient condition	Maximum hydraulic yield	Improvement factor
R2	GPK1	$9{\cdot}10^{-4}$	$7.7{\cdot}0^{-3}$	8.6
	GPK2	$2{\cdot}10^{-1}$	n/a	n/a
R3	GPK1	$5{\cdot}10^{-4}$	$1.7{\cdot}0^{-2}$	28.3
	GPK2	$3{\cdot}0^{-4}$	$1.6{\cdot}10^{-2}$	53.3
R5	GPK2	$2{\cdot}10^{-4}$	$1{\cdot}10^{-2}$	50
	GPK3	n/a	$3.9{\cdot}10^{-3}$	n/a
	GPK4	$1{\cdot}0^{-4}$	$5{\cdot}10^{-3}$	50

4.2. Analysis of hydraulic testing and stimulation characteristics

With the aim to further investigate major hydraulic characteristics of stimulation operations, we have analysed the volume, the flow rates and the differential pressure at stationary condition of the hydraulic test experiments (see Annex A). Herein, only those data have been analysed that refer to hydraulic stimulation tests that are not perturbed by massive chemical stimulation. The effectiveness of chemical stimulations is discussed by Nami et al. (2008).

Under these premises testing of GPK4 is excluded since most stimulations in this well are of chemical nature as well as experiments carried out after the 2005 long-term circulation in R5, which also involved strong chemical reactants. However, the analyses include stimulations 03FEB12 in GPK2 and 03JUN27 in GPK3 with weak chemical additives (0.18–0.45% HCl). Furthermore, results from the 95AUG15 test are excluded due to clogging by injection of cuttings. Effects from the two long-term circulation tests are treated at the end of this section. From all tests conducted in all Soultz reservoirs, 40 are considered in the following three analyses. Due to different number of acquired data for the individual tests, each of the three analyses account also for a different number of tests. For instance, the five-step test 95JUN16 is included five times in a pressure to flow rate analysis, but only one time in a maximum volume analysis. The total single-test volume for the considered experimental subset ranges from 4 m^3 to 34,000 m^3.

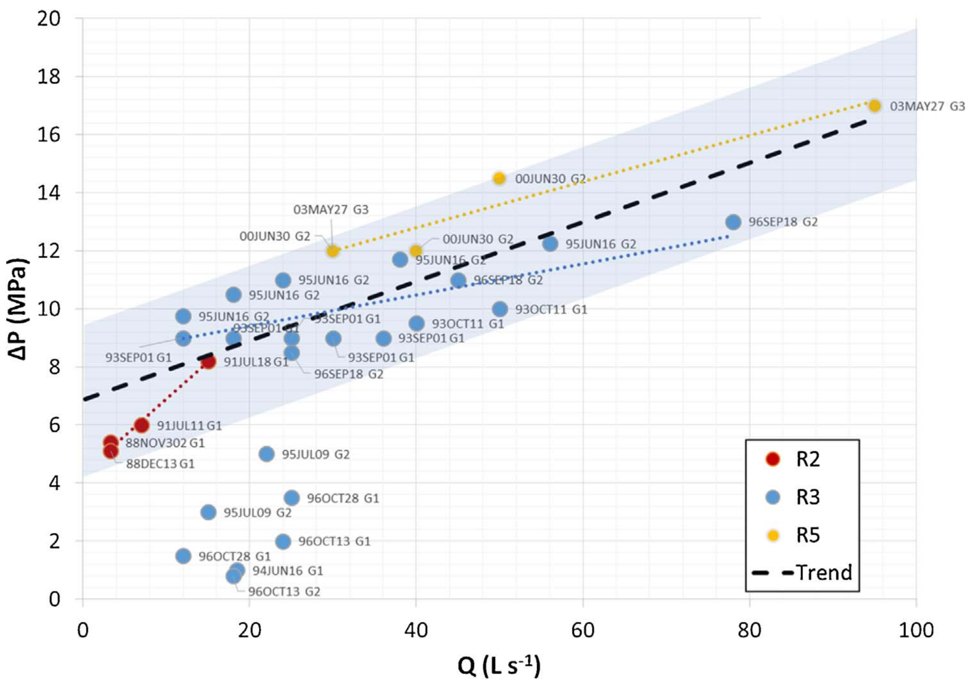

Fig. 7. Flow rate Q and differential pressure ΔP for the high (blue) and low (red) total single-test volumes for 88NOV302 (GPK1, R2), 88DEC13 (GPK1, R2), 91JUL11 (GPK1, R2), 91JUL18 (GPK1, R2), 96OCT13 (GPK1, GPK2, R3), 93OCT11 (GPK1, R3), 00JUN30 (GPK2, R5), 93SEP01 (GPK1, R3), 95JUL09 (GPK2, R3), 96SEP18 (GPK2, R3), 95JUN16 (GPK2, R3), 03MAY27 (GPK3, R5) (ordered by increasing total single-test volume.The reservoir specific and overall regression lines with overall $\Delta P = 0.102\ \text{MPa}\ L^{-1}\ s^{-1} \cdot Q + 6.86\ \text{MPa}$ ($R^2 = 0.72$) represents a fit without the outliers for 94JUN16, 95JUL09, 96OCT13 and 96OCT28. (For interpretation of the references to colour in this figure legend, the reader is referred to the web version of this article.)
Data source: see Annex A.

The single-step injections at comparably low flow rates between 3 and 15 L s^{-1} in R2 caused comparably low differential pressures with a mean value of about 5 MPa. A trend of increasing differential pressure with increasing flow rate is observed (Jung, 1992). The experiments in R3 and R5 generally involved higher flow rates. They were mostly conducted using a multi-step scheme and include those experiments that lead to high improvement factors (see Section 4.1). As expected, the mean differential pressure in this group of experiments is generally higher than in R2, and shows a larger variability. Fig. 7 (blue dots) illustrates the flow rate ranging between 12 L s^{-1} (93SEP01) and typically up to 60 L s^{-1}, and up to > 90 L s^{-1} (03MAY27). The differential pressures in the reservoir range between 8 and 13 MPa (17 MPa peak value). Besides individual trends in R2 to R5, a general trend between flow rate and differential pressure of 0.1 MPa s L^{-1} can be identified for all three wells and reservoirs (Fig. 7). Around this regression line most experiments range at ΔP = ± 2.2 MPa, being characterized in Fig. 7 by a grey shaded area representing approximately a ± 30% variation of differential pressure. It can be stated that the reservoir performance in R3 and R5 shows the expected behaviour of increasing pressure with fluid flow rate. Given this general linear trend, it needs to be noted that other analyses have identified a nonlinear nature of individual test sequences in post-stimulation tests,

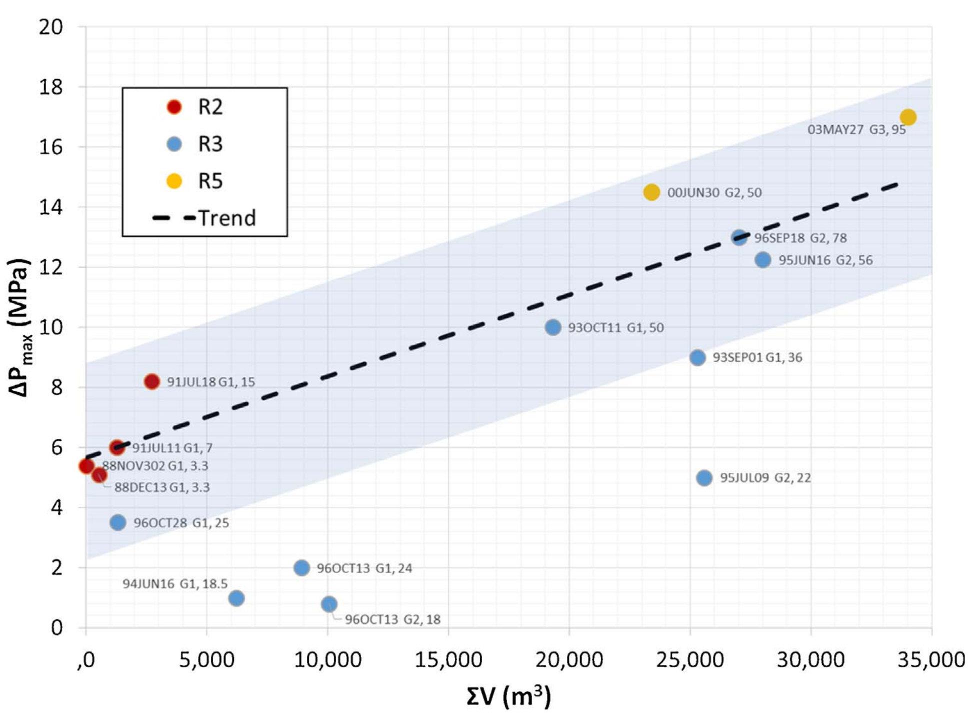

Fig. 8. Total single-test volume, ΣV and maximum differential pressure ΔP_{max} for the high (blue) and low (red) total single-test volumes at the Soultz EGS site. Last value in the data label indicates the maximum flow rate. The regression line is calculated without the outliers for 94JUN16, 95JUL09 and 96OCT13 with $\Delta P_{max} = 3 \cdot 10^{-4}\ \text{MPa}\ m^{-3} \cdot \Sigma V + 5.67\ \text{MPa}$ ($R^2 = 0.85$). (For interpretation of the references to colour in this figure legend, the reader is referred to the web version of this article.)
Data source: see Annex A.

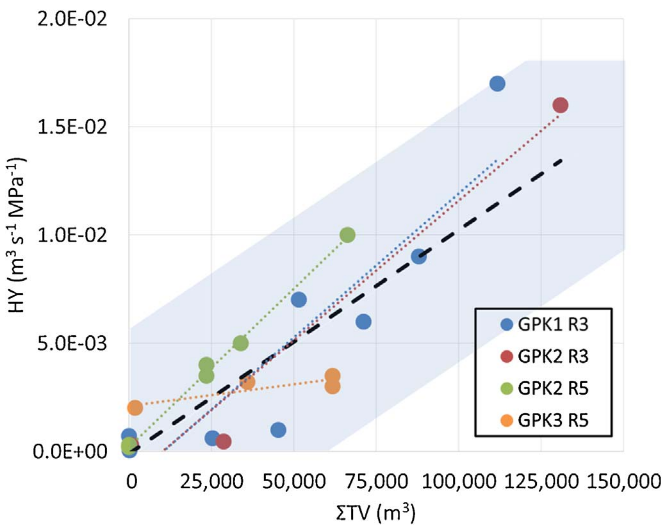

Fig. 9. Hydraulic yields, HY, obtained from stimulation and test experiments in wells GPK1, GPK2 in R3 and GPK2 and GPK3 in R5 versus the total fluid flow volume ΣTV (Data: see Annex A). Data include experiments and the tests of 93MAY27 to 95AUG01 (GPK1, R3), 95FEB10 to 95JUN16 and 96OCT13 (GPK2, R3), 99OCT13 to 03JUN24 (GPK2, R5), 03MAR11 to 04AUG17 (GPK3, R5). Well and reservoir specific as well as the overall regression with overall HY = 10^{-7} $m^3\,s^{-1}MPa^{-1}$ · ΣTV (R^2 = 0.77) include all data point. Similar behaviour can be deduced from R2 (not shown).

especially for R3 (Kohl et al., 1997) that can only be evaluated by more detailed data interpretation.

The outliers in Fig. 7 with much lower differential pressures versus flow rate are observed for 94JUN16, 95JUL09, 96OCT13, and 96OCT28. Except for 96OCT13, these are post-stimulation circulation tests and represent the highest hydraulic yields. The experiments and injection schemes for 95JUN16 and 96OCT13 will be described in detail in Section 4.3.

In order to cross-check the link between differential pressure and flow rate, the relation between maximum differential pressures and total single-test volumes is shown in Fig. 8. A pressure increase with test volume of about $\Delta P_{max} = 3{\cdot}10^{-4}$ MPa m^{-3}·ΣV + 5.67 MPa defines an upper bound trend. It is controlled mainly by tests with maximum flow rates of ≤ 15 L s^{-1} into GPK1 in R2 and between 50 and 95 L s^{-1} into R3 and R5. Total single-test volumes that were injected at flow rates between about 18 and 25 L s^{-1} (94JUN16, 95JUL09, 96OCT13, and 93SEP01 tests) show reduced maximum differential pressures.

The presented linear trends are derived at test periods when the initial transient pressure build-up has reached saturation (at about 6 MPa) and at which hydro-mechanical interaction impedes a continuation of the initial pressure increase. Interestingly, this observation compares nicely with the seismic observations in R3 when noticeable e seismicity started at approx. ΔP > 3 MPa (Baria et al., 2004).

For a refined analysis for each reservoir, i.e., the hydraulic yield, accounting for PI and JI, as a function of total fluid flow volume is studied. Fig. 9 illustrates the trend of increasing hydraulic yield with increasing total injected volume for the individual reservoirs and the overall site. While the trends for the wells GPK1 and 2 in R3 and R5 are rather similar, the increase in hydraulic yield in GPK3 is significantly lower. A linear trend with a mean gradient of 10^{-7} $m^3\,s^{-1}$ MPa ^{1} per m^{-3} is observed across the different wells and reservoirs.

In summary, the outliers (96OCT13 and 95JUN16 with the corresponding test 95JUL09) indicate promising structures with low-pressure increase that could have key importance for mitigating seismic hazard. Indeed, maximum moment magnitudes from downhole sensors of Mw = 0.1 in 1995 and Mw = 0.3 in 1996 (Gerard et al., 1997) are by up to one order of magnitude lower compared to all other stimulations (Emmanuel Gaucher, pers. comm., 2015).

The general linear trend between hydraulic yield and total fluid flow volume suggests that the total amount of fluid that was flowed through a well interval correlates positively with the performance of the Soultz reservoir. Against this background, the long-term circulation experiments 97JUL12 in R3 and 05JUL11 in R5 were accounted for, too. In both experiments, GPK2 was operated as a producer allowing for a quantification of PI_{GPK2}. During 97JUL12 when GPK1 was used as an injector, a total single-test volume of ΣV ≈ 244000 m^3 was circulated during 125 days. During 05JUL11 when GPK3 was used as an injector with GPK4 being an additional producer, a total single-test volume of ΣV ≈ 165000 m^3 was produced in GPK2, representing 80% of the total production during the test. Comparing the corresponding hydraulic yields of these two tests to the data presented in Fig. 9 highlights a similar pattern: the PIs of GPK2 in R3 (red dots in Fig. 9) drops from a maximum of 0.016 $m^3\,s^{-1}$ MPa^{-1} to 0.008 $m^3\,s^{-1}$ MPa^{-1} at the end of the 97JUL12 experiment. In R5 (green dots in Fig. 9), they decrease from a maximum of 0.01–0.009 $m^3\,s^{-1}$ MPa^{-1} in 05JUL11. Correspondingly, JI of GPK3 (orange dots in Fig. 9) decreases slightly from 0.0035 to 0.0025 $m^3\,s^{-1}$ MPa^{-1} in 05JUL11. Both large-volume circulation experiments point therefore to a stable or even slightly decreasing hydraulic yield. Such behaviour has been attributed to thermo-hydraulic effects caused by heating (Jung, 1999). This effect will be investigated further when analysing the operational data.

4.3. Progressive cyclic injection experiments

In contrast to conventional injection experiments with a continuous or stepwise changing flow rate, these experiments include alternating sequences of injection and pressure recovery possibly combined with a progressive change in flow rate. Concepts of cyclic injection in oil reservoirs are a standard tool to improve recovery rates (e.g., Monger et al., 1991). It is however beyond standard application to geothermal reservoirs. Progressive cyclic injection in EGS has been approximated first during the 93SEP01 hydraulic stimulation of GPK1 in R3 (e.g., Evans et al., 2005). After having stepped up injection to 12 L s^{-1}, four subsequent steps up to 36 L s^{-1}, with short (few hours) shut-in intervals, have been applied. These intervals led to a decrease in wellhead pressure by a maximum of 7 MPa. Since 93SEP01 was targeted specifically for improving the lower permeable structures with the most permeable fractures sanded off the result of this progressive cyclic injection scheme cannot be directly compared to the success of 95JUN16.

Although carried out with the intention to measure instantaneous shut-in pressure before starting the next step, the injection scheme in the 95JUN16 experiment approaches best modern stimulation concepts. It is shown in Fig. 4 with six flow steps, each with durations of 1–2 days, with flow rates increasing up to 56 L s^{-1}. The total pressure reached values 42 and 45 MPa during this test. The success of this experiment was revealed by a post-stimulation step-injection test 95AUG01 when GPK1 and GPK2 had nearly identical hydraulic characteristics with approximately 20 L s^{-1} injected at an overpressure of 3.5 MPa (Baumgartner et al., 1996). This is significantly lower than the critical pressure for fracture propagation.

Such injection schemes were also later used in other geothermal wells such as in GtLa2 at Landau (Schindler et al., 2010). In the TH1 Genesys well at Hannover (Germany) a modification of the “huff-puff” concept was applied (Tischner et al., 2010). The observations during 95JUN16 agree with the nearby Landau site when a PI of 0.01 $m^3\,s^{-1}$ MPa^{-1} was obtained also by progressive cyclic injection at peak flow rates of up to 190 L s^{-1} (Schindler et al., 2010). Furthermore, progressive cyclic stimulation concepts have gained interest by showing a reduction of both, the total number of induced seismic events, as well as the occurrence of larger magnitude events. This is explained by the concept of fatigue hydraulic fracturing (Zang et al., 2017), and is in agreement with the observation of reduced maximum magnitude (see Section 4.2) and the smaller number of seismic events (5000 to 6000) registered by downhole sensors (Gerard et al., 1997) compared to nearly 20,000 downhole events in the 1993 stimulations, also registered by downhole sensors (Jones et al., 1995).

It may be noted here that a detailed evaluation of pressure versus flow curves will result in a better understanding of the physical processes involved. As such, non-linear effects with identical flow to pressure patterns arise from step-injection (94JUL04, 95JUL01, 96SEP29) and production (94JUN16) tests in R2 (Kohl et al., 1996; Kohl and Rybach, 2001). The validity of this observation, i.e. non-Darcian flow, is typically restricted to pressures < 3 MPa in GPK1 and < 6 MPa in GPK2 and confirmed over four hydraulic steps. Permeability enhancement seems to start at pressures above these critical values. Original analyses had indicated that complex hydraulic flow regimes are not restricted to near-well vicinities, but rather extend large distances until reaching high capacity far-field faults (Kohl et al., 1997).

5. Operational reservoir behaviour

The operational phase of the Soultz EGS project started in 2008 and is conducted mostly combining R3 and R5. Herein, operation will be analysed until 2013 when a major restructuring of the Soultz project began (Table 3). During this period, the operation took place over 55% of the time with nine individual operation cycles ranging from a short operation periods of 31 days up to a long operation interval of 323 days. Annex B provides an overview of the total 1.4 million m^3 circulated.

Apart from 2008 to 2009, when an additional 12 L s^{-1} were produced from GPK4, GPK2 was the only production well. During operation, circulation was maintained using different pump configurations. Production at GPK2 was accomplished with a line shaft pump first installed at 350 m depth and then reinstalled at 250 m for the second and follow-up tests. GPK4 was equipped with an electrical submersible pump mounted at 500 m depth. Both are operating at maximum pressure of about 2 MPa. The produced fluid was cooled at the surface using a secondary cooling system and re-injected into GPK3 using one of the two surface injection pumps with a minimum pressure of 4.7 MPa (Genter et al., 2012). Injection into GPK1 was integrated into the circulation since the 09MAR01 experiment only using gravity. Since the 11JAN05 experiment, re-injection into GPK3 was carried out without a surface injection pump. A key objective in the operation phase was to prevent major seismic events and to monitor the seismic response as a function of injection pressure (e.g., Cuenot et al., 2011). Unfortunately, with the exception of 10NOV15 (Schindler et al., 2010) and 11AUG08 (Genter et al., 2011c) no further detailed evaluation of the hydraulic situation in Soultz was conducted. This restriction only allows us to draw preliminary conclusions.

GPK2 acted mostly as an injector until April 2003, and was continuously used as a producer thereafter. Fig. 10 depicts this situation and the evolution of the apparent hydraulic yield in R5. As noted earlier, the stimulations of GPK2 (00JUN30 and 03FEB12) have increased the JI up to 0.005 $m^3\ s^{-1}\ MPa^{-1}$. The subsequent PI supported by the stimulation 03MAY27 turned to be a factor of two higher, leading to $PI_{R5,G2}$ of about 0.01 $m^3\ s^{-1}\ MPa^{-1}$ that was achieved during the long-term circulation test 03JUN24 and reproduced in 05JUL11, two years later. With the change from JI to PI a bias may be introduced to the hydraulic yield values due to buoyancy effects that is not accounted for. Therefore, we consider these values as maximum hydraulic yields. These maximum values can be compared to the only available PI data on the two operation cycles (10NOV15 and 11AUG08) that appear to be twice this value after being in operation for a total of 793 days. Under the premises that this increase is due to a reservoir improvement, we may relate this to an increase rate per total fluid flow volume of about $1.0 \cdot 10^{-8}\ m^3\ s^{-1}\ MPa^{-1}$ per m^3. This value would be in contrast with the earlier observation (see Section 4.2) of a hydraulic saturation around GPK2 during 05JUL11. As a consequence, these values will be discussed below.

The importance of a casing leakage as a cause of the increasing hydraulic yield of GPK2 has been discussed (e.g., Jung et al., 2010). When GPK2 was cased down to 4403 m the earlier openhole section of the R3 was cased off. After the loss of a logging tool, a casing restriction was detected at about 3890 m depth, next to the depth of well deviation

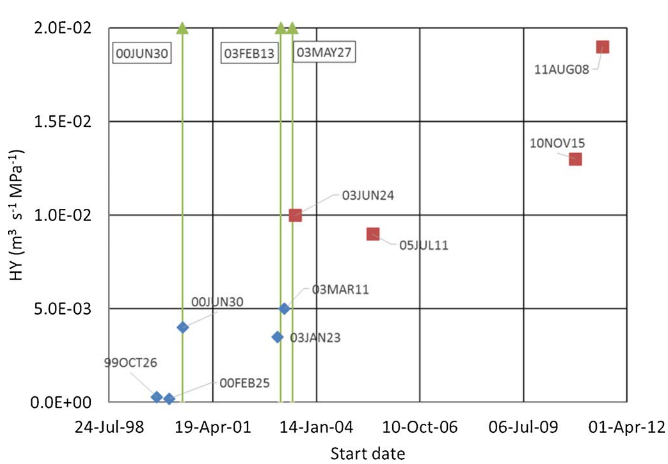

Fig. 10. Evolution of GPK2 HY, JI until 03MAR11 and PI starting from 03JUN24, in the R5 measured during single-well injection tests (blue) and circulation production tests (red). Note that despite the low-volume production in GPK3, the test 03MAR11 has been classified injection test here. Hydraulic stimulation is indicated in green. (For interpretation of the references to colour in this figure legend, the reader is referred to the web version of this article.)
Data source: see Annex A and Annex B.

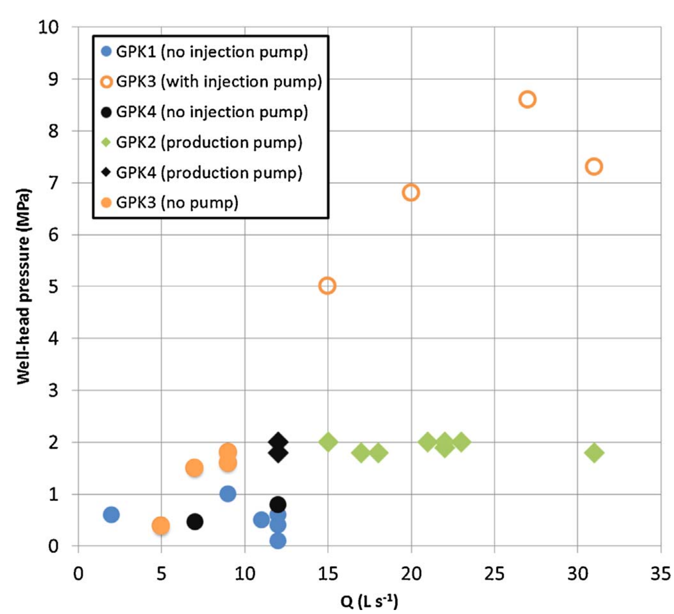

Fig. 11. Operational data of GPK1 (blue), GPK2 (green), GPK3 (orange) and GPK4 (black) in R5 with mean injection (circle) and production (diamond) rates over the different operation periods and mean wellhead pressure between 2008 and 2013 at the wellheads of GPK1 to GPK4. Full/open circles indicate operation without/with injection pump. (For interpretation of the references to colour in this figure legend, the reader is referred to the web version of this article.)
Data source: see Annex B.

and opposite to a fault zone at the bottom of R3. Pfender et al. (2006) proposed three major flow zones in the inaccessible deeper part of GPK2 using a brine displacement analyses from the low-rate injection test 06MAR13. Two flow zones are located below the casing shoe taking about 85% of the flow whereas one with a contribution of > 15% of the total flow is postulated to be at 3860 m within the cased section (Jung et al., 2010; Pfender et al., 2006). Assuming constant leakage over time with a contribution of > 15%, a minimum contribution to the hydraulic yield between JI = $8{\cdot}10^{-4}$ and PI = $1.5{\cdot}10^{-3}\ m^3\ MPa^{-1}\ s^{-1}$ can be calculated. Jung et al. (2010) concluded that instantaneous reaction to pressure changes indicates the influence of the near-well domain rather than from the fracture zone aligned with this leak. Given the JI increase in Fig. 10 and the brine displacement analyses relating JI to pre-operational conditions, a first-order assessment indicates that the contribution of the casing leak and of the reservoir are of the same magnitude.

Lacking further hydraulic analysis of operational data, e.g., using borehole simulators such as Nusiaputra et al. (2016), we outline here the hydraulic behaviour in terms of wellhead pressure and flow rate. Fig. 11 combines the different values for the three R5 wells and the R3 GPK1 well. In the wells GPK2 and partly GPK4 (during the period 2008–2009), fluid was produced at flow rates between 8 and 31 L s^{-1} and wellhead pressure of 2 MPa fixed by the line shaft pump. With the aim of reducing seismicity to a minimum, the injection wells GPK1, GPK3 and GPK4 (period 2012–2013) have been operated at minimum pressure inferred from the wellhead observations. As such, flow rates ≤ 12 L s^{-1} with typically wellhead pressures of < 1 MPa had been used for GPK1 and GPK4. In contrast, injection in GPK3 at low flow rates ≤ 9 L s^{-1} caused higher wellhead pressures of 1.8 MPa. With the injection pump at GPK3 being off during most of the operation, we may extrapolate a linear increase of wellhead pressure with flow rate by a gradient of a = 0.31 MPa s L^{-1}. It may be noted that this value would agree with the earlier history of GPK3 in 2008–2010 when wellhead pressures of up to 8.7 MPa at 27 L s^{-1} were reached.

In summary, it is indicated from wellhead data that GPK1 and GPK4 reveal a better JI compared to GPK3. The apparent, most positive performance of GPK2 during operations is questionable due to effects of buoyancy and borehole integrity, and must be addressed by more sophisticated techniques such as borehole simulators.

6. Conclusions

The development of the three Soultz reservoirs took place over more than 20 years. The investigations during this period allowed for key EGS technology findings concerning geological, hydraulic, thermal and mechanical conditions. The presented experimental review illustrates the engineering learning curve achieved in Soultz. Although it is restricted to a first-order assessment of hydraulic effects ignoring these interactions their implications are obvious: As such, the various high-flow fracture zones correlate with alteration zones and slip tendency. Furthermore, the injection pressure during operation was limited to reduce seismic hazard. However, this compilation indicates clear patterns of the hydraulic behaviour at Soultz.

From this perspective, the different phases of reservoir development highlight the experience gained on hydraulic stimulation. Despite all stimulation efforts, the high natural hydraulic performance of the shallow R2 reservoir observed in GPK2 remains unique. Low injection rates into GPK1 (R2) demonstrate the feasibility of hydraulic stimulating less permeable zones. At the R3 reservoir flow rate was drastically increased. Finally, R5 being developed as a triplet EGS operation started with observation of induced seismicity. The presented review indicates clear trends for effective hydraulic stimulation experiments carried out at this worldwide unique EGS reference site. Our analyses reveal that:

- With the exception of GPK2 in R2 and GPK3 in R5, the initial hydraulic conditions from single-well injection tests are comparable to each other in the three reservoirs. Thus, this allows for a comparison of the effectiveness of different stimulation measures.
- The case study of R3 reveals that JI and PI are comparable in the initial phase of stimulation. They differ, however, by orders of magnitude in a more mature hydraulic setting.
- During stimulation, hydraulic yield appears to be enhanced most effectively using cyclic injection schemes in combination with circulation. This is confirmed in follow-up EGS projects e.g., in Landau. Its advantage is a significantly low injection volume.
- Volume appears to be key driving factors for enhancing hydraulic conditions of Soultz. The effect seems to be more important during hydraulic stimulation compared to circulation at low flow rates. Typically moderate flow rate, long-term circulation experiments do contribute less significantly to improving hydraulic yields. The long-term behaviour over several years can be analysed only using borehole simulations that infer reservoir condition from wellhead data.

In all the above statements borehole integrity plays an important role. After many years of testing there are unfortunately now several borehole sections inaccessible for logging or any other operations. This may be caused by mechanical instability of the rock matrix during stimulation. A safe implementation of hydraulic stimulation is crucial for production from EGS reservoirs.

In the last years, the production in Soultz was optimized for reducing induced seismicity during operation. It was achieved by reducing the injection wellhead pressure leading to a reduction in production flow rates by almost 50%. For the further development of EGS to economic levels, this learning curve needs to be continued by applying controlled high-flowrate injection.

Finally, this compilation presents a starting basis for future research in fractured rock that should target more extensive conceptual models of this most intensive and documented site. This first assemblage of the hydraulic performance in Soultz provides key aspects to design and engineer EGS performance at other locations.

Acknowledgements

The authors acknowledge the GEIE EMC for providing Soultz borehole test data and for the financial support to start the project. Part of this work has been carried out in the framework of the Labex G-Eau-Thermie Profonde, which is co-funded by the French government under the program "Investissements d'Avenir". Finalization of the project is funded through the HelmholtzPortfolio project *Geoenergy* and the *H2020 DEEPEGS* project. We would like to thank Dr. Reinhard Jung for fruitful discussions. The authors appreciate the helpful and constructive comments of the reviewers Drs. Marcelo J. Lippmann and Trenton T. Cladouhos and the managing editor Dr. Sabodh Garg.

Annex A. Overview of the hydraulic and chemical stimulations in the three reservoir levels R2, R3, R5 at the Soultz-sous-Forêts EGS site. When the number of multi-steps is > 5, they are grouped in five major steps. Standard letters: Single-well, italic letters: circulation tests; grey shaded: PI or JI > $7{\cdot}10^{-3}$ m^3 MPa^{-1} s^{-1} (starting day of testing is always given). References are given, where available for publically available documents: 1: Jung (1992), 2: Jung et al. (1996), 3: Baria et al. (1995), 4: Jung (1999), 5: Jung et al. (1995), 6: Gérard et al. (1997), 7: Baria et al. (1998), 8: Baria et al. (2000), 9: Weidler (2001), 10: Nami et al. (2008), 11: Tischner et al. (2007), 12: Schindler et al. (2008), 13 : Hettkamp et al. (2004), 14: Gérard et al. (2006).

	Stimulation	Ref.	Well	Depth (mMD)	Hydraulic yield (m^3 MPa^{-1} s^{-1})	JI / PI	Total single-test volume (m^3) + : injection - : production	Chemical additives [concentration (%)]	Total fluid flow volume (m^3)	Step I Flow rates (l s^{-1})	Step I Δp (MPa)	Step I Approx. duration (h)	Step II Flow rates (l s^{-1})	Step II Δp (MPa)	Step II Approx. duration (h)	Step III Flow rates (l s^{-1})	Step III Δp (MPa)	Step III Approx. duration (h)	Step IV Flow rates (l s^{-1})	Step IV Δp (MPa)	Step IV Approx. duration (h)	Step V Flow rates (l s^{-1})	Step V Δp (MPa)	Step V Approx. duration (h)
Res2	88NOV302	1	GPK1	1966–2000		JI	3.7		3.7	3.3	5.4	50												
	88DEC13	1	GPK1	1966–2000	9.0E-04	JI	524		527.7	3.3	5.1	50												
	91JUL11	1	GPK1	1966–2000	2.2E-03	JI	1250		1778	7.0	6	50												
	91JUL18	1	GPK1	1966–2000	7.7E-03	JI	2700		4478	15.0	8.5–7.9	50												
	95FEB02	2	GPK2	2100	2.0E-01	JI	618		618	8.3														
Res3.5	93MAY27	2	GPK1	3560–3590	7.0E-04	PI	41		82															
	93AUG19	3,4	GPK1	3560–3590	5.0E-04	JI	105		1115	6.0		packer faillure												
	93SEP01	5,4	GPK1	2850–3400	5.0E-05	JI	25300		26415	0.15 − 12	< 9	105												
	93SEP01	5,4	GPK1	2850–3400	6.0E-04	JI	25300		26415				18.0	< 9	48	25.0	< 9	48	30.0	< 9	48	36.0	< 9	78
	93OCT01	3,4	GPK1	3457–3507			580		26995	3.5		packer faillure												
	93OCT11	5,4	GPK1	2850–3590	1.0E-03	JI	19300		46295	40.0	9.5	96	50.0	10	24									
	94JUN16	5	GPK1	2850–3590	7.0E-03	PI	−6200		52495	11.0 − 18.5	1	24	5.0		168	11.0 − 18.5		60						
	94JUL04	5	GPK1	2850–3590			9600		62095	6.0		36	12.0		72	18.0		84						
	95JUN10	6,4	GPK2	3211–3876	3.0E-04	JI	75		75	30.0		6.5												
	95JUN14	6,4	GPK2	3211–3876			624		699	30.0		6.5												
	95JUN16	6,4	GPK2	3211–3876		JI	28000	(300 heavy brine)	28699	12.0	9.75	54	18.0	10.5	48	24.0	11	48	38.0	11.7	48			
	95JUN16	6,4	GPK2	3211–3876		JI	28000		28699													56.0	12.25	24
	95JUN16	6,4	GPK1	2850–3590	6.0E-03	PI	−10000		72095	13.0		240												
	95JUL01	2	GPK2	3211–3876	4.5E-03	JI	2200		30899															
	95JUL09	4	GPK2	3211–3876			25570		54269	15.0	3	144	22.0	5	216									
	95JUL09	4	GPK1	2850–3590	1.7E-02	PI	−16900		88995	15.0		144												
	95AUG01	4	GPK2	3211–3876			21780		76049	21.3		216												
	95AUG01	4	GPK1	2850–3590	9.0E-03	PI	−23760		112755	21.3		216												
	95AUG15	4	GPK2	3211–3876			4420		80469	15.0	5.5	96												
	95AUG15	4	GPK1	2850–3590	2.6E-03	PI	−4130		116885	10.0		72												
	96AUG14	4	GPK2	3211–3876	1.4E-02	PI	n/a		80469															
	96SEP18	6,4	GPK2	3211–3876	6.0E-03	JI	27004		107473	25.0	8.5	66	45.0	11	48	78.0	13	48						
	96SEP18	6,4	GPK1	2850–3590			−3700		120585	12.0		80												
	96SEP29	2	GPK2	2850–3590			13300		120773	6.2		24	15.0		36	25.0		48	37.5		48			
	96OCT13	6,4	GPK1	3211–3876	8.0E-03	JI	8900		129485	12.0 − 24.0	2	144												
	96OCT13	6,4	GPK2	2850–3590	1.6E-02	PI	−10055		130828	18.0	0.8	168												
	96OCT28	6,4	GPK1	3211–3876			1305		130790	12.0	1.5	27	25.0	3.5	2									
	96OCT28	6,4	GPK2	2850–3590			−1500		132328	15.0		27												
	97JUL12	7,4	GPK1	3211–3876			244000	Aquaprox	374790	25.0		2940												
	97JUL12	7,4	GPK2	2850–3590	1.3E-02	PI	−244000		376328	25.0		2940												
Res5	99OCT26	8	GPK2	4431–5084	3.0E-04	PI	n/a																	
	00FEB25	9	GPK2	4431–5084	2.0E-04	JI	n/a																	
	00JUN30	10,11,12	GPK2	4431–5084	4.0E-03	JI	23400		23400	30.0	12	24	40.0	12	27	50.0	14.5	90						
	03JAN23	13	GPK2	4431–5084	3.5E-03	JI	9150		32550	15.0		168												
	03FEB12	10,11	GPK2	4431–5084		JI	5814	[0,18; 0,18; 0,09 HCl]	38364	15.0 − 30.0		96												
	03MAR11	11	GPK2	4431–5084	5.0E-03	JI	8950		47314	15.0		24	30.0		72									

03MAR11	11	GPK3	4558–5090	2.0E-03	PI	−1890		1890	5.0		144							
03MAY27	10,11	GPK3	4558–5090	3.2E-03	JI	34000		35890	20.0−30.0	12	72	50.0−95.0*	17	120	20.0−25.0	60		
03MAY27	10,11	GPK2	4431–5084		JI	3400		50714	25.0		36							
03JUN11	13	GPK2	4431–5084		PI	−4000		54714	10.0		132							
03JUN24	13	GPK2	4431–5084	1.0E-02	PI	−25000		79714	15.0		384							
03JUN24	13	GPK3	4558–5090		JI	25000		60890	15.0		384							
03JUN27	10,11	GPK3	4558–5090		JI	865	[0,45 HCl]	61755	20.0		12							
04AUG17	11	GPK3	4558–5090	3.5E-03	JI	n/a		61755										
04AUG18	11	GPK3	4558–5090	3.0E-03	JI	n/a		61755										
04SEP08	11	GPK4	4746–5250	1.0E-04	PI	n/a												
04SEP13	10,11	GPK4	4746–5250	2.0E-03	JI	9300		9300	30.0−45.0	16	84							
05FEB07	10,11	GPK4	4746–5250		JI	12300		21600	30.0		24	45.0		48	25.0	24		
05FEB22	10	GPK4	4746–5250	2.0E-03	JI	4500		26100	10.0		24	15.0		24	25.0	24		
05MAR02	10	GPK4	4746–5250		JI	5200	[0,2 HCl]	31300	27.0	19	48							
05MAR13	10	GPK4	4746–5250	3.0E-03	JI	n/a		31300										
05JUL11	14	GPK2	4431–5084	9.0E-03	PI	−165000		244714	12.0		4200							
05JUL11	14	GPK3	4558–5090	2.5E-03	JI	205000		266755	15.0−20.0		4150							
05JUL11	14	GPK4	4746–5250	2.5E-03	PI	−40000		71300	3.0		3850							
06APR24	10	GPK4	4746–5250	3.0E-03	JI													
06MAY17	10	GPK4	4746–5250		JI	4225	[0,15; 0,12 HCl; 0,03 HF]		18.0−28.0		24	22.0		6	22.0−28.0	22		
06MAY29	10	GPK4	4746–5250	4.0E-03	JI													
06OCT19	10	GPK4	4746–5250		JI	5100	[NaOH; 0,19 Na3NTA]		24.0		53	35.0		1.6	40.0			
06OCT25	10	GPK4	4746–5250	4.0E-03	PI													
07JAN29	10	GPK4	4746–5250	3.0E-03	JI													
07FEB07	10	GPK3	4558–5090	3.5E-03	JI													
07FEB15	10	GPK3	4558–5090		JI	2770	[0,05-0,1C6H8O7; 0,001-0,01 HF; 0,005-0,015HBF4; 0,01-0,05 NH4Cl]		35.0		12	55.0		1.5	45.0	12	30.0	22
07MAR12	10	GPK3	4558–5090	3.9E-03	JI													
07MAR21	10	GPK4	4746–5250		JI	2770	[0,05-0,1C6H8O7; 0,001-0,01 HF; 0,005-0,015HBF4; 0,01-0,05 NH4Cl]		30.0		6	55.0		1.5	40.0	1.5	35.0	6
07MAR21	10	GPK4	4746–5250	5.0E-03	PI													

*95 L s^{-1} only in peaks.

Annex B. Overview of the circulation experiments in the deep reservoir levels III at the Soultz-sous-Forêts EGS site (Data sources: Cuenot et al., 2011; Genter et al., 2011a, 2011b, 2011c; Genter et al., 2013; Melchert et al., 2010; Schindler, 2009). Injections without surface pump are indicated in grey. HY : hydraulic yield ; Δp : pressure difference between undisturbed reservoir pressure at 4700 m and pressure of the water column.

Well / Year	Period	Producers / Injectors	Maximum flow rate (L s^{-1})	Maximum well-head pressure (MPa)	Total single-circulation volume (m^3)	Duration of test (d)	Mean Δp (MPa)	Mean HY (m^3 MPa^{-1} s^{-1})
2008								
GPK2	08JUL08-08AUG17	Prod.	31	1.8	62000	40		
GPK3		Inj.	31	7.3				
GPK2	08NOV24-08DEC17	Prod.	17	1.8	63000	40		
GPK3	08NOV17-08DEC17	Inj.	27	8.6				
GPK4	08NOV17-08DEC20	Prod.	12	1.8				< 5.0E-3
2009								
GPK1	09MAR01-09OCT16	Inj.	9	1	285000	230		
GPK2	09MAR01-09OCT16	Prod.	22	2				
GPK3	09MAR01-09OCT16	Inj.	20	6.8				
GPK4	09MAY19-09OCT16	Prod.	12	2		150		
2009–2010								
GPK1	09NOV29-10OCT14	Inj.	2	0.6	500000	323		
GPK2	09NOV17-10OCT14	Prod.	18	1.8				
GPK3	09NOV25-10OCT14	Inj.	15	5				
2011								
GPK1	11JAN05-11APR06	Inj.	11	0.5	165000	90		
GPK2	11JAN03-11APR06	Prod.	22	1.9			16.5	1.3E-02
GPK3	11JAN05-11APR06	Inj.	9	1.8			25.9	3.6E-03
GPK1	11AUG08-11OCT21	Inj.	12	0.4	135000	70		
GPK2	11AUG08-11OCT21	Prod.	23	2			12.1	2.0E-02
GPK3	11AUG08-11OCT14	Inj.	9	1.6			25.5	3.7E-03
2012								
GPK1	12MAR27-12APR27	Inj.	12	0.1	30000	31		
GPK2	12MAR27-12APR27	Prod.	21	2				
GPK3	12MAR27-12APR27	Inj.	7	1.5				
GPK4	12MAR27-12APR27	Inj.	12	0.8				
2013								
GPK1	13JAN15-13MAR28	Inj.	12	0.6	200000	180		
GPK2	13JAN15-13JUL15	Prod.	15	2				
GPK3	13JAN15-13JUL15	Inj.	5	0.38				
GPK4	13JAN15-13JUL15	Inj.	7	0.46				

References

Agemar, T., Schellschmidt, R., Schulz, R., 2012. Subsurface temperature distribution in Germany. Geothermics 44, 65–77.

Aquilina, L., Pauwels, H., Genter, A., Fouillac, C., 1997. Water-rock interaction processes in the Triassic sandstone and the granitic basement of the Rhine Graben: geochemical investigation of a geothermal reservoir. Geochim. Cosmochim. Acta 61 (20), 4281–4295.

Aquilina, L., Rose, P., Vaute, L., Brach, M., Gentier, S., Jeannot, R., Jacquot, E., Audigane, P., Tran-Vie, T., Jung, R., Baumgärtner, J., Baria, R., Gerard, A., 1998. A tracer test at the Soultz-Sous-Forets Hot Dry Rock geothermal site. In: Proceedings 23rd Workshop on Geothermal Reservoir Engineering. Stanford University, Stanford, California. pp. 343–350.

Aquilina, L., de Dreuzy, J.R., Bour, O., Davy, P., 2004. Porosity and fluid velocities in the upper continental crust (2–4 km) inferred from injection tests at the Soultz-sous-Forêts geothermal site. Geochim. Cosmochim. Acta 68 (11), 2405–2415.

Bächler, D., Kohl, T., Rybach, L., 2003. Impact of graben-parallel faults on hydrothermal convection—Rhine Graben case study. Physics and Chemistry of the Earth, Parts A/B/C 28, 431–441.

Baillieux, P., Schill, E., Edel, J.-B., Mauri, G., 2013. Localization of temperature anomalies in the Upper Rhine Graben: insights from geophysics and neotectonic activity. Int. Geol. Rev. 55, 1744–1762.

Baillieux, P., Schill, E., Abdelfettah, Y., Dezayes, C., 2014. Possible natural fluid pathways from gravity pseudo-tomography in the geothermal fields of Northern Alsace (Upper Rhine Graben). Geotherm. Energy J. 2 (1), 14pp.

Baria, R., Garnish, J., Baumgartner, J., Gérard, A., Jung, R., 1995. Recent developments in the European HDR research programme at Soultz-sous-Forêts (France). In: Proceedings, World Geothermal Congress. Florence, Italy. pp. 2631–2637.

Baria, R., Baumgärtner, J., Gérard, A., Jung, R., 1998. European hot dry rock geothermal research programm 1996–1997 final report. EHDRA. Kutzenhausen 155pp.

Baria, R., Baumgärtner, J., Gérard, A., Garnish, J., 2000. The European HDR programme: main targets and results of the deepening of the well GPK2 to 5000 m. In: Proceedings, World Geothermal Congress. Beppu-Morioka Japan. pp. 3643–3652.

Baria, R., Michelet, S., Baumgärtner, J., Dyer, B., Gerard, A., Nicholls, J., Hettkamp, T., Teza, D., Soma, N., Asanuma, H., 2004. Microseismic monitoring of the world's largest potential HDR reservoir. In: Proceedings, 29th Workshop on Geothermal Reservoir Engineering. Stanford University, Stanford, California. (8pp.).

Baujard, C., Bruel, D., 2006. Numerical study of the impact of fluid density on the pressure distribution and stimulated volume in the Soultz HDR reservoir. Geothermics 35, 607–621.

Baujard, C., Genter, A., Dalmais, E., Maurer, V., Hehn, R., Rosillette, R., Vidal, J., Schmittbuhl, J., 2017. Hydrothermal characterization of wells GRT-1 and GRT-2 in rittershoffen, France: implications on the understanding of natural flow systems in the rhine graben. Geothermics 65, 255–268.

Baumgartner, J., Jung, R., Gérard, A., Baria, R., Garnish, J., 1996. The European HDR project at Soultz sous forets: Stimulation of the second deep well and first circulation experiments. Socomine, Route de Kutzenhausen, Soultz sous Forets, FR; Bundesanstalt fur Geowissenschaften und Rohstoffe, Stilleweg, Hannover, DE; DGXII, European Commission, Brussels, 328pp.

Baumgartner, J., Gerard, A., Baria, R., Jung, R., Tran-Vieta, T., Gandyn, T., Aquilina, L., Garnish, J., 1998. Circulating tha HDR reservoir at Soultz: maintaining production and injection flow in complete balance – initial results of the 1997 circulation experiment. In: Proceedings 23rd Workshop on Geothermal Reservoir Engineering. Stanford University, Stanford, California. pp. 11–20.

Bear, J., 1972. Dynamics of Fluids in Porous Media. American Elsevier, New York, N.Y (780pp).

Beauce, A., Jones, R., Fabriol, H., Twose, C., Hulot, C., 1992. Microseismic monitoring of hydraulic experiments undertaken during phase II of the Soultz HDR project (Alsace, France), Report No. SGP-TR-141-37. BRGM/IMRG, Orleans Cedex, FR; CSMA, Rosemanowes Quarry, Herniss, Penryn, Cornwall, UK, 141pp.

Cuenot, N., Frogneux, M., Dorbath, C., Calo, M., 2011. Induced microseismic activity during recent circulation tests at the EGS site of Soultz-sous-Forêts (France). In: Proceedings 36th Workshop on Geothermal Reservoir Engineering. Stanford University, Stanford, Califoria. (13pp.).

Dezayes, C., Genter, A., Hooijkaas, G.R., 2005. Deep-seated geology and fracture system of the EGS Soultz reservoir (France) based on recent 5 km depth boreholes. In: Proceedings, World Geothermal Congress. Antalya, Turkey. (6pp).

Dezayes, C., Genter, A., Valley, B., 2010. Structure of the low permeable naturally fractured geothermal reservoir at Soultz. C.R. Geosci. 342, 517–530.
Evans, K.F., Genter, A., Sausse, J., 2005. Permeability creation and damage due to massive fluid injections into granite at 3.5 km at Soultz: 2. Critical stress and fracture strength, Journal of Geophysical Research. Solid Earth 110 (B4). http://dx.doi.org/10.1029/2004JB003169.
Gérard, A., Baumgärtner, J., Baria, R., Jung, R., 1997. Géothermie: retour d'expérience de Soultz-sous-Forêts. Mémoires de la Société géologique de France 172, 43–52.
Gérard, A., Genter, A., Kohl, T., Lutz, P., Rose, P., Rummel, F., 2006. The deep EGS (enhanced geothermal system) project at soultz-sous-Forêts (Alsace, France). Geothermics 35, 473–483.
Garg, S.K., Combs, J., 1997. Use of slim holes with liquid feedzones for geothermal reservoir assessment. Geothermics 26, 153–178.
Garnish, J., 2002. European activities in Hot Dry Rock research,.In Energy, U.S.D.o. (Ed.), Open Meeting on Enhanced Geothermal Systems, Reno (Nevada), 8–9.
Geiermann, J., Schill, E., 2010. 2-D Magnetotellurics at the geothermal site at Soultz-sous-Forêts: resistivity distribution to about 3000 m depth. C. R. − Geosci. 342, 587–599.
Genter, A., Traineau, H., Dezayes, C., Elsass, P., Ledesert, B., Meunier, A., Villemin, T., 1995. Fracture analysis and reservoir characterization of the granitic basement in the HDR Soultz project (France). Geotherm. Sci. Technol. 4, 189–214.
Genter, A., Homeier, G., Chevremont, P., Tenzer, H., 1999. Deepening of GPK-2 HDR borehole, 3880–5090 m, (Soultz-sous-Forêts, France) geological monitoring. BRGM Open File Report 77pp.
Genter, A., Guillou-Frottier, L., Feybesse, J.-L., Nicol, N., Dezayes, C., Schwartz, S., 2003. Typology of potential hot fractured rock resources in Europe. Geothermics 32, 701–710.
Genter, A., Cuenot, N., Goerke, X., Melchert, B., Moeckes, W., Scheiber, J., 2011. Programme de suivi scientifique et technique de la centrale géothermique de Soultz pendant l'exploitation (Rapport d'avancement Phase III: activité 2011. GEIE Exploitation Minière de la Chaleur, Kutzenhausen, France, 73pp.
Genter, A., Cuenot, N., Goerke, X., Moeckes, W., Schieber, J., 2011. Scientific and technical activity of the Soutz geothermal power plant (Progress Report from Dec 2010 to June 2011). GEIE Exploitation Minière de la Chaleur, Kutzenhausen, France, 62pp.
Genter, A., Cuenot, N., Goerke, X., Moeckes, W., Schieber, J., 2011. Scientific and technical activity of the Soutz geothermal power plant (Progress report from July to November 2011), Kutzenhausen, France, 72pp.
Genter, A., Cuenot, N., Goerke, X., Bernd, M., Sanjuan, B., Scheiber, J., 2012. Status of the Soultz geothermal project during exploitation between 2010 and 2012. In Proceedings 37th Workshop on Geothermal Reservoir Engineering, Stanford University, California, 12pp.
Genter, A., Cuenot, N., Melchert, B., Moeckes, W., Ravier, G., Sanjuan, B., Sanjuan, R., Scheiber, J., Schill, E., Schmittbuhl, J., 2013. Main achievements from the multi-well EGS Soultz project during geothermal exploitation from 2010 and 2012. In Proceedings, European Geothermal Conference, Pisa, Italy, 10pp.
Grecksch, G., Ortiz, A., Schellschmidt, R., 2003. Thermophysical study of GPK2 and GPK3 granite sampes GGA report. GGA, Institute, Hannover, Germany (33pp).
Guillou-Frottier, L., Carrè, C., Bourgine, B., Bouchot, V., Genter, A., 2013. Structure of hydrothermal convection in the Upper Rhine Graben as inferred from corrected temperature data and basin-scale numerical models. J. Volcanol. Geotherm. Res. 256, 29–49.
Hettkamp, T., Baumgärtner, J., Baria, R., Gerard, A., Gandy, T., Michelet, S., Teza, D., 2004. Electricity production from hot rocks, In proceedings, 29th workshop on geothermal reservoir engineering, stanford university, standford. California 26–28.
IEA, 2011. Technology Roadmap: Geothermal Heat and Power. In: Agency, I.E. (Ed.). International Energy Agency, Paris, France, 52pp.
Illies, H.J., Greiner, G., 1979. Holocene movements and state of stress in the rhinegraben rift system. Tectonophysics 52, 349–359.
Ingebritsen, S.E., Manning, C.E., 1999. Geological implications of a permeability-depth curve for the continental crust. Geology 27, 1107–1110.
Jahn, M., Breunig, M., Butwilowski, E., Kuper, P.V., Thomsen, A., Al-Doori, M., Schill, E., 2017. Temporal and Spatial Database Support for Geothermal Sub-surface Applications. In Advances in 3D Geoinformation. Springer International Publishingpp. 337–356.
Jones, R., Beauce, A., Jupe, A., Fabriol, H., Dyer, B., 1995. Imaging induced microseismicity during the 1993 injection tests at Soultz-sous-Forets France. In: Proceedings, World Geothermal Congress. Florence, Italy. pp. 2665–2669.
Jung, R., Willis-Richard, J., Nicholls, J., Bertozzi, A., Heinemann, B., 1995. Evaluation of hydraulic tests at Soultz-sous-Forêts, European HDR Site. In: Proceedings, World Geothermal Congress. Florence, Italy. pp. 2671–2676.
Jung, R., Cornet, F., Rummel, F., Willis-Richards, J., 1996. Hydraulic stimulation results 1992/1993. In: Baria, R., Baumgärtner, J., Gérard, A. (Eds.), European Hot Dry Rock Programme 1992–1995. EHDRA, Kutzenhausen, France, pp. 328.
Jung, R., Schindler, M., Nami, P., Tischner, T., 2010. Determination of flow exits in the Soultz borehole GPK2 by using the brine displacement method. C. R. Geosci. 342, 636–643.
Jung, R., 1992. Hydraulic fracturing and hydraulic testing in the granitic section of the borehole GPK1, Soultz sous Forets. In: Bresee, J.C. (Ed.), Geothermal Energy in Europe: The Soultz Hot Dry Rock Project. Gordon and Breach Science Publishers, Washington, USA, pp. 149–198.
Jung, R., 1999. Erschließung permeabler Rißzonen für die Gewinnung geothermischer Energie aus heißen Tiefengesteinen. GGA-Institut, Hannover, 82pp.
Jung, R., 2013. EGS –Goodye or back to future. In: Bunger, A.P., McLennan, J., Jeffrey, R. (Eds.), Intech, 95-121.
Kohl, T., Rybach, L., 2001. Assessment of HDR reservoir geometry by inverse modelling Of non-laminar hydraulic flow. In: Proceedings, 26th Workshop on Geothermal Reservoir Engineering, Stanford University. Stanford, California. pp. 29–31.
Kohl, T., Jung, R., Hopkirk, R., Rybach, L., 1996. Non-linear flow transients in fractured rock masses-the 1995 injection experiment in Soultz. In: Proceedings, 21st Workshop onr Geothermal Reservoir Engineering, Stanford University. Stanford, California. pp. 157–164.
Kohl, T., Evans, K., Hopkirk, R., Jung, R., Rybach, L., 1997. Observation and simulation of non-Darcian flow transients in fractured rock. Water Resour. Res. 33, 407–418.
Kohl, T., Bächler, D., Rybach, L., 2000. Steps towards a comprehensive thermo-hydraulic analysis of the HDR test site Soultz-sous-Forêts. In: Proceedings, World Geothermal Congress. Beppu_Morioka, Japan. pp. 2671–2676.
Kolditz, O., 2002. Computational Methods in Environmental Fluid Mechanics, vol. 649 Springer, Berlin. http://dx.doi.org/10.1007/978-3-662-04761-3. (378pp).
Meller, C., Kontny, A., Kohl, T., 2014. Identification and characterization of hydrothermally altered zones in granite by combining synthetic clay content logs with magnetic mineralogical investigations of drilled rock cuttings. Geophys. J. Int. 199 (1), 465–479.
Monger, T., Ramos, J., Thomas, J., 1991. Light oil recovery from cyclic CO2 injection: influence of low pressures impure CO2, and reservoir gas. SPE Reservoir Eng. 6, 25–32.
Nami, P., Schellschmidt, R., Schindler, M., Tischner, T., 2008. Chemical stimulation operations for reservoir development of the deep crystalline HDR/EGS system at Soultz-sous-Forêts (France). In: Proceedings 32nd Workshop on Geothermal Reservoir Engineering, Stanford University. Stanford, California. pp. 28–30.
Nusiaputra, Y., Dimier, A., Kohl, T., 2016. A two-phase geothermal wellbore-simulator to model THC behaviour using Elmer-Phreeqc. In: European Geothermal Congress 19.-23.10. Strasbourg, France. 4pp.
O'Sullivan, M., Pruess, K., 1980. Ananlysis of injection testing of geothermal reservoirs. Report LBL-10985; CONF-800920-22. California University, Berkeley (USA). Lawrence Berkeley Laboratory, 4pp.
Pfender, M., Nami, P., Tischner, T., Jung, R., 2006. Status of the Soultz deep wells based on low rate hydraulic tests and temperature logs. In: EHDRA Scientific Conference 15.-16.06. Soultz-sous-Forêts, France. 12 pp.
Place, J., Diraison, M., Naville, C., Géraud, Y., Schaming, M., Dezayes, C., 2010. Decoupling of deformation in the upper rhine graben sediments: seismic reflection and diffraction on 3-component vertical seismic profiling (Soultz-sous-Forêts area). C.R. Geosci. 342, 575–586.
Pribnow, D., Schellschmidt, R., 2000. Thermal tracking of upper crustal fluid flow in the Rhine Graben. Geophys. Res. Lett. 27, 1957–1960.
Pribnow, D.F.C., 2000. The deep thermal regime in Soultz and implications for fluid flow, GGA Report. GGA Institut. Hannover 9pp.
Rummel, F., König, E., 1991. Density, ultrasonic velocities and magnetic susceptibility measurements on the core material from borehole EPS1 at Soultz-sous-Forêts. Internal report. Ruhr-Universität, Bochum 58pp.
Sanjuan, B., Pinault, J.-L., Rose, P., Gérard, A., Brach, M., Braibant, G., Crouzet, C., Foucher, J.-C., Gautier, A., Touzelet, S., 2006. Tracer testing of the geothermal heat exchanger at Soultz-sous-Forêts (France) between 2000 and 2005. Geothermics 35, 622–653.
Schellschmidt, R., Clauser, C., 1996. The thermal regime of the Upper Rhine Graben and the anomaly at Soultz. Zeitschrift für Angewandte Geologie 42, 40–44.
Schindler, M., Nami, P., Schellschmidt, R., Teza, D., Tischner, T., 2008. Summary of hydraulic stimulation operations in the 5 km deep crystalline HDR/EGS reservoir at Soultz-sous-Forêts. In Proceedings 33th Workshop on Geothermal Engineering, Stanford University, Stanford, California, 9pp.
Schindler, M., Baumgärtner, J., Gandy, T., Hauffe, P., Hettkamp, T., Menzel, H., Penzkofer, P., Teza, D., Tischner, T., Wahl, G., 2010. Successful Hydraulic Stimulation Techniques for Electric Power Production in the Upper Rhine Graben, Central Europe, In Proceedings, World Geothermal Congress, Bali, Indonesia, 7pp.
Schindler, M., 2009. Hydraulic data recorded during the three circulations with downhole pumps at Soultz. GEIE Exploitation Minière de la Chaleur, Kutzenhausen, France, 26pp.
Stober, I., Bucher, K., 2007. Hydraulic properties of the crystalline basement. Hydrol. J. 15, 213–224.
Tischner, T., Schindler, M., Jung, R., Nami, P., 2007. HDR project Soultz: Hydraulic and seismic observations during stimulation of the 3 deep wells by massive water injections. In Proceedings, 32nd Workshop on Geothermal Engineering, Stanford University, Stanford, California, 7pp.
Tischner, T., Evers, H., Hauswirth, H., Jatho, R., Kosinowski, M., Sulzbacher, H., 2010. New concepts for extracting geothermal energy from one well: the GeneSys-Project. In: Proceedings, World Geothermal Congress. Bali, Indonesia. pp. 25–30.
Vidal, J., Genter, A., Schmittbuhl, J., 2015. How Permeable Fractures in the Triassic Sediments of Northern Alsace Characterize the Top of Hydrothermal Convective Cells? Characterization of Deep Geothermal Systems, 3:8, 10.1186/s40517-015-0026-4, Evidences from Soultz geothermal boreholes (France), Geothermal Energy, Special Issue.
Weidler, R., Oates, S., Dyer, B., Baumgartner, J., Gérard, A., 2002. Integrated microseismic and hydraulic monitoring of HDR reservoir stimulation, Soultz, France.I n Proceedings, 27th Workshop on Geothermal Engineering, Stanford University, Stanford, California, 6pp.
Weidler, R., 2001. Slug test in the non-stimulated 5 km deeep well GPK2, Internal report. BGR, Hannover, Germany, 20pp.
Zang, A., Stephansson, O., Stenberg, L., Plenkers, L., Specht, s., Milkereit, C., Schill, E., Kwiatek, G., Dresen, G., Zimmermann, G., Dahm, T., Weber, M., 2017. Hydraulic fracture monitoring in hard rock at 410 m depth with an advanced fluid-injection protocol and extensive sensor array. Geophysical.